

15 SEISMIC MARGINS ANALYSIS

Table of Contents

15.1 INTRODUCTION	15.1-1
15.2 METHODOLOGY	15.2-1
15.2.1 Assumptions.....	15.2-1
15.3 SEISMIC FRAGILITIES.....	15.3-1
15.3.1 Overview.....	15.3-1
15.3.2 Fragility Formulation.....	15.3-1
15.3.3 Structural Fragility.....	15.3-3
15.3.3.1 Reactor Building Complex Structures	15.3-4
15.3.3.2 RCCV and RPV Pedestal.....	15.3-11
15.3.3.3 RPV Support Brackets	15.3-12
15.3.3.4 Control Building Structure.....	15.3-13
15.3.4 Component Fragility.....	15.3-13
15.3.5 Fragility Summary.....	15.3-14
15.4 ACCIDENT SEQUENCE HCLPF ANALYSIS	15.4-1
15.4.1 Full Power Analysis.....	15.4-1
15.4.1.1 Full Power Seismic Event Tree.....	15.4-1
15.4.1.2 System Analysis.....	15.4-2
15.4.2 Shutdown Analysis	15.4-4
15.4.2.1 Shutdown Seismic Event Tree	15.4-4
15.4.2.2 System Analysis.....	15.4-6
15.5 RESULTS	15.5-1
15.6 INSIGHTS	15.6-1
15.7 CONCLUSIONS.....	15.7-1
15.8 REFERENCES	15.8-1

List of Tables

Table 15-1	Seismic Capacity Summary	15.8-2
Table 15-2	Seismic Fragility for Reactor Building Shear Walls.....	15.8-3
Table 15-3	Seismic Fragility for Containment Wall	15.8-4
Table 15-4	Seismic Fragility for RPV Pedestal.....	15.8-5
Table 15-5	Seismic Fragility for RPV Support Brackets	15.8-6
Table 15-6	Seismic Fragility for Control Building	15.8-7
Table 15-7	ESBWR Systems and Components/Structures Fragilities	15.8-8
Table 15-8	Seismic Event Tree Nodal HCLPF Equations	15.8-10
Table 15-9	HCLPF Derivation for Figure 15-3a and Figure 15-3b	15.8-11
Table 15-10a	HCLPF Derivation for Figure 15-17a, Figure 15-18 and Figure 15-19.....	15.8-12
Table 15-10b	HCLPF Derivation for ESBWR Shutdown Seismic Event Tree Sequences For Figure 15-17b	15.8-13

List of Figures

Figure 15-1. Typical Fragility Curves 15.8-14

Figure 15-2. Horizontal Single Envelope Design and Performance-Based Seismic
Design Spectra of ESBWR..... 15.8-15

Figure 15-3a. Seismic Event Tree (Full Power)..... 15.8-16

Figure 15-3b. Seismic Induced Break Outside Containment in RWCU Line (Full
Power)..... 15.8-17

Figure 15-4. Structural Seismic Fault Tree (Full Power) 15.8-18

Figure 15-5. DC Power Seismic Fault Tree..... 15.8-19

Figure 15-6. SCRAM Seismic Fault Tree..... 15.8-20

Figure 15-7. SRV Seismic Fault Tree..... 15.8-21

Figure 15-8. SLCS Seismic Fault Tree..... 15.8-22

Figure 15-9. IC Seismic Fault Tree..... 15.8-23

Figure 15-10. DPV Seismic Fault Tree..... 15.8-24

Figure 15-11. GDCS Seismic Fault Tree..... 15.8-25

Figure 15-12. VB Seismic Fault Tree 15.8-26

Figure 15-13. PCCS Seismic Fault Tree..... 15.8-27

Figure 15-14. PI Seismic Fault Tree 15.8-28

Figure 15-15. FPW Seismic Fault Tree 15.8-29

Figure 15-16. Structural Seismic Fault Tree (Shutdown Conditions) 15.8-30

Figure 15-17a. Seismic Event Tree – Shutdown Mode 5 and Mode 5 Open 15.8-31

Figure 15-17b. Seismic Event Tree – Shutdown Mode 5 and Mode 5 Open
(Sensitivity)..... 15.8-32

Figure 15-18. Seismic Event Tree – Shutdown Mode 6 Unflooded..... 15.8-33

Figure 15-19. Seismic Event Tree – Shutdown Mode 6 Flooded..... 15.8-34

Figure 15-20. BOC In RWCU Line Fault Tree 15.8-35

15 SEISMIC MARGINS ANALYSIS

This section documents the PRA-based seismic margin analysis of the ESBWR.

15.1 INTRODUCTION

The seismic risk analysis is performed to assess the impacts of seismic events on the safe operation of the ESBWR plant.

A PRA-based Seismic Margins Analysis (SMA) is performed for the ESBWR using the systems models and the fragility analysis method of Ref. 15-1 to calculate High Confidence Low Probability of Failure (HCLPF) accelerations for important accident sequences and accident classes.

The analysis shows that the ESBWR plant is capable of withstanding an earthquake of at least 1.67 times the Safe Shutdown Earthquake (SSE) with a high confidence of low probability of failure.

The scope of the analysis includes both at-power and shutdown seismic-induced accident scenarios.

15.2 METHODOLOGY

The seismic risk assessment uses a Seismic Margins Analysis (SMA) method based on Ref. 15-1 and 15-2 to calculate High Confidence Low Probability of Failure (HCLPF) seismic capacities for important accident sequences and accident classes.

The PRA-based seismic margins approach used in this analysis evaluates the capability of the plant to withstand an earthquake of 1.67 times the Safe Shutdown Earthquake (1.67*SSE).

The analysis involves the following two major steps:

- (1) Seismic fragilities
- (2) Accident sequence HCLPF analysis

The seismic fragilities of the ESBWR systems, structures, and components are based on generic industry information and ESBWR specific seismic capacity calculations for certain structures.

The MIN-MAX method is used in the determination of functional and accident sequence fragilities. Per the MIN-MAX method, the overall fragility of a group of inputs combined using OR logic (i.e., seismic event tree nodal fault tree) is determined by the lowest (minimum) HCLPF input. Conversely, per the MIN-MAX method, the overall fragility of a group of inputs combined using AND logic (i.e., seismic event tree sequence) is determined by the highest (maximum) HCLPF input.

Both at-power and shutdown seismic-induced accident scenarios are analyzed.

15.2.1 Assumptions

- Structural dimensions and various input factors to the fragility section's formulations are assumed.
- Prior to detailed design information becoming available, minimum values of one and two-thirds times SSE are assumed for components HCLPF values.
- COLA actions are required to verify plant specific HCLPF.
 - As-built engineering walk-down is required to verify assumptions made in SMA.
 - Components may require strengthening if as-built SMA indicates additional capacity margin is required.

15.3 SEISMIC FRAGILITIES

15.3.1 Overview

This subsection presents seismic capacities for selected structures and components that have been identified as potentially important to the seismic risk analysis of the ESBWR standard plant. The seismic capabilities are first estimated in terms of seismic fragilities, from which the high confidence of low probability of failure (HCLPF) capacities are then derived. The HCLPF capacities serve as input to the system analysis following the seismic margins approach.

The peak ground acceleration of the design earthquake is 0.5g for the Safe Shutdown Earthquake (SSE). Extensive seismic soil-structure interaction analyses of the reactor/fuel building complex and control building were performed for a wide range of generic site conditions under a 0.5g single envelope design spectra. This single envelope design spectra is a composite of Reg. Guide 1.60 spectra anchored to 0.3g and to the North Anna ESP design spectra anchored to 0.5g. The analysis results, in terms of site-envelope SSE loads, are presented in Appendix 3A of the ESBWR DCD Tier 2 Rev. 4 (Ref. 15-3). The standard plant designed to these site-envelope seismic loads may result in significant design margins when it is situated at a specific site, particularly a soft soil site. Thus, the seismic capacities estimated from the site-envelope design requirements may be very conservative for certain sites; however, confirmation of margins must be done for as-built conditions.

For the seismic category I structures for which seismic design information is available, the seismic fragilities are evaluated using the Separation-of-Variable method in Ref. 15-1. This approach identifies various conservatisms and associated uncertainties introduced in the seismic design process (both capacity and demand sides) and provides a probabilistic estimate of the earthquake level required to fail a structure or component in a postulated failure mode by extrapolating from the design information supplemented by limited nonlinear analysis to account for building response beyond yielding.

For safety-related components such as pumps, valves, and electrical equipment whose design details are not currently available, a generic HCLPF capacity of 1.67*SSE is assigned. This generic HCLPF is considered to be “reasonably achievable” for the ESBWRs designed to the single envelope design spectra for a wide range of sites.

15.3.2 Fragility Formulation

Seismic fragility of a structure or component is defined herein to be the cumulative conditional probability of its failure as a function of the mean peak ground acceleration (i.e., the average of the peak of the two horizontal components).

The probability model adopted for fragility description is the lognormal distribution. Using the lognormal distribution assumption, an entire family of fragility curves can be fully described in terms of the median ground acceleration and two random variables as:

$$A = A_m \epsilon_\gamma \epsilon_\mu \quad (15.3-1)$$

Where:

A_m = median peak ground acceleration corresponding to 50% failure probability.

- ϵ_γ = a lognormally distributed random variable accounting for inherent randomness about the median. It is characterized by unit median and logarithmic standard deviation β_γ .
- ϵ_μ = a lognormally distributed random variable accounting for uncertainty in the median value. It is characterized by unit median and logarithmic standard deviation β_μ .

With known values of A_m , β_γ , and β_μ , the failure probability P_f at acceleration less than or equal to a given acceleration a can be computed using the following equation for any non-exceedance probability (NEP) level Q .

$$P_f(A \leq a|Q) = \Phi \left[\frac{1}{\beta_\gamma} \ln \left(\frac{a}{A_m} \right) + \frac{\beta_\mu}{\beta_\gamma} \phi^{-1}(Q) \right] \quad (15.3-2)$$

Where Φ is the standard Gaussian cumulative distribution function. Figure 15-1 shows a typical family of fragility curves for various NEP levels. The center solid curve represents the median fragility curve at 50% NEP level. The logarithmic standard deviation of the randomness component β_γ determines the curve slope. The logarithmic standard deviation of the uncertainty component β_μ is a measure of the spread from the median curve. The 95th percentile and 5th percentile curves in Figure 15-1 are the upper and lower bounds of the failure probability for a given acceleration, corresponding to 95% and 5% NEP levels, respectively.

When only the point estimate is of interest, which is the case for this analysis, the total variability about the median value is taken to be the square root of the sum of the squares (SRSS) of the inherent randomness and uncertainty components.

$$\beta_c = \sqrt{\beta_\gamma^2 + \beta_\mu^2} \quad (15.3-3)$$

The fragility curve corresponding to the median value A_m with associated composite logarithmic standard deviation can be computed by the following equation:

$$P_f(A \leq a) = \Phi \left[\frac{1}{\beta_c} \ln \left(\frac{a}{A_m} \right) \right] \quad (15.3-4)$$

This composite fragility curve is also called the mean fragility curve and is shown as the dashed curve in Figure 15-1 for illustration. It represents the best estimate fragility description.

In estimating the median ground acceleration capacity and the associated variability, an intermediate variable defined as safety factor F is utilized. The safety factor is related to the median ground acceleration capacity by the following relationship.

$$A_m = FA_d \quad (15.3-5)$$

Where A_d is the ground acceleration of the reference design earthquake to which the structure or component is designed. A key step in the seismic fragility estimate thus involves the evaluation of the factor of safety associated with the design for each important potential failure mode. The design margins inherent in the component capacity and the dynamic response to the specific acceleration are the two basic considerations. Each of the capacity and response margins involves several variables, and each variable has a median factor of safety and variability

associated with it. The overall factor of safety F is the product of the factor of safety for each variable F_i .

$$F = \prod_i F_i \quad (15.3-6)$$

The overall composite logarithmic standard deviation is SRSS of the composite logarithmic standard deviations in the individual factors of safety.

$$\beta_c = \sqrt{\sum_i \beta_{ci}^2} \quad (15.3-7)$$

Knowing the median peak ground acceleration (A_m) and associated logarithmic standard deviation (β_c); the HCLPF capacity is obtained using the equation below.

$$\text{HCLPF} = A_m \exp(-2.326\beta_c) \quad (15.3-7a)$$

15.3.3 Structural Fragility

The plant structures are divided into two categories according to their function and the degree of integrity required to protect the public during a seismic event. These categories are seismic category I and non-category I. Seismic category I includes those structures whose failure might cause or increase the severity of an accident, which would endanger the public health and safety. The reactor building and control building structures are in this category. The non-category I structures are those structures which are important to reactor operation, but are not essential for preventing an accident which would endanger the public health and safety, and are not essential for the mitigation of the consequences of these accidents. One example is the turbine building structure.

For the purpose of this study, structures are considered to fail functionally when inelastic deformations of the structure under seismic load increase to the extent that the operability of the safety-related components attached to the structure cannot be assured. The drift limits chosen for structures are estimated as corresponding to the onset of significant structural damage. For many potential modes of failure, this is believed to represent a conservative bound on the level of inelastic structural deformation that might interfere with the function of the system housed within the structure.

The potential of seismic-induced soil failure such as liquefaction, differential settlement, or slope instability is highly site dependent and cannot be assessed for generic site conditions. It is assumed in this analysis that there is no soil failure potential in the range of ground motions considered.

Building-to-building impact due to differential building displacements under strong earthquakes is deemed not credible since a sufficient distance to avoid impact separates adjacent buildings. Differential building displacements of sufficient magnitude could, however, potentially result in damage to interconnecting piping, depending on system configuration and sliding resistance of building foundation. Detailed evaluation of seismic capacities of interconnecting systems against differential building displacement cannot be made due to lack of design details and specific site conditions. It is assumed that the mode of failure due to differential building displacement has a capacity no less than the required margin of 1.67*SSE.

15.3.3.1 Reactor Building Complex Structures

Detailed fragility evaluations were made for the following structures in the reactor building (RB) and fuel building (FB) complex. The RB and FB share the same basement and are fully integrated. The term "reactor building" when mentioned hereafter also includes the structures of the fuel building. As for the containment structure, it is enclosed by and integrated into the RB.

- Building shear walls
- Containment wall (upper drywell and wetwell)
- RPV pedestal (same as lower drywell wall)
- RPV support brackets

Those structures were evaluated according to the approach outlined previously and using various safety factors as presented below.

The factor of safety for a structure against a specific failure mode is the product of the capacity factor F_c and structural response factor F_{rs} ;

$$F = F_c F_{rs} \quad (15.3-8)$$

The individual factors, the capacity factor and the response factor, are discussed in the following subsections.

15.3.3.1.1 Capacity Factor (F_c)

The capacity factor represents the capability of a structure to withstand seismic excitation in excess of the design earthquake. This factor is composed of two parts:

$$F_c = F_s F_u \quad (15.3-9)$$

Where:

F_s = the ultimate structural strength margin above the design SSE load, and

F_u = the inelastic energy absorption factor accounting for additional capacity of the structure to undergo inelastic deformations beyond yield.

The capacity estimated by this approach is the elastic capacity equivalent to the actual nonlinear behavior under strong motion earthquakes.

Strength Factor (F_s)

The strength factor associated with seismic load can be calculated using the following equation.

$$F_s = \frac{P_u - P_n}{P_s} \quad (15.3-10)$$

Where:

P_u = the actual ultimate strength,

P_n = the normal operating loads, and

P_s = the design SSE load.

The earthquake-resistant structural elements of the reactor building are reinforced concrete shear walls that are integrated with the reinforced concrete cylindrical containment through concrete floor slabs. The specified compressive strength of concrete is 34.5 MPa for the building and 27.5 MPa for the mat. The specified yield strength of ASTM A615, Grade 60 reinforcing steel is 414 MPa. These are design values; the actual material strengths are higher.

Concrete compressive strength used for design is normally specified as a value at a specific time after mixing (28 or 90 days). This value is verified by laboratory testing of mix samples. The strength must meet specified values, allowing a finite number of failures per number of trials. There are two major factors that affect the actual strength:

- a. To meet the design specifications, the contractor attempts to create a mix that has an “average” strength somewhat above the design strength, and
- b. As concrete ages, it increases in strength.

Taking those two elements into consideration, the actual compressive strength of aged concrete is commonly 1.3 times the design strength (Ref. 15-8). The total logarithmic standard deviation about the median strength is about 0.13.

According to the same reference, the ratio of the median yield strength to the specified strength of reinforcing steel is taken to be 1.2 with logarithmic standard deviation of 0.12.

The median yield strength of steel plates is typically 1.25 times the code specified strength with logarithmic standard deviation of 0.14 (Ref. 15-8 and 15-9).

The reactor building shear wall is chosen as an example for the discussion of the strength factor evaluation. For reinforced concrete shear walls the ultimate shear strength can be computed using the following equation (Reference 15-1).

$$\begin{aligned}
 v_u &= v_c + v_s \\
 &= 8.3\sqrt{f'_c} - 3.4\sqrt{f'_c}\left(\frac{h}{w} - \frac{1}{2}\right) + \frac{N}{4wt} + \rho_{se}f_y
 \end{aligned}
 \tag{15.3-11}$$

Where:

- v_u = ultimate shear strength
- v_c = shear strength provided by concrete
- v_s = shear strength provided by reinforcing steel
- f'_c = concrete compressive strength
- h = wall height
- w = wall length

- N = bearing load
- f_y = yield strength of reinforcing steel
- t = wall thickness
- ρ_{se} = $A\rho_v + B\rho_h$
- ρ_h = horizontal steel reinforcement ratio
- ρ_v = vertical steel reinforcement ratio
- A & B = constants depending on h/w:

	A	B
$h/w < 0.5$	1	0
$0.5 \leq h/w < 1.5$	$1.5 - h/w$	$h/w - 0.5$
$1.5 < h/w$	0	1

In computing ultimate shear strength with this equation, the median material strengths of the concrete and reinforcing steel defined above are used and the wall bearing load is conservatively neglected.

The strength factor F_s is then calculated using Equation 15.3-10 for each of the levels of the reactor building shear walls. The normal operating loads do not result in lateral force and horizontal loads induced by SRV actuations are found to be negligible compared to the SSE-induced horizontal loads. Therefore, the strength factor is the ratio of the median shear strength to the design SSE shear. The lowest strength factor is found to be 1.82. This is calculated for the generic medium soil stiffness site condition that has the highest calculated seismic response. The associated logarithmic standard deviation is calculated to be 0.01 using the second moment approximation (Ref. 15-10) accounting for both concrete and reinforcing steel material strength variability. There is also an uncertainty associated with Equation 15.3-11 since it is an approximate model fit to data. The modeling uncertainty is 0.20 expressed in terms of logarithmic standard deviation (Ref. 15-1). The total composite logarithmic standard deviation in the median strength factor is 0.20, which is the SRSS value of 0.01 for the material strength uncertainty and 0.20 for the equation uncertainty. Flexural failure of the wall is found to have higher strength factor, therefore, shear failure is the governing mode of failure.

Inelastic Energy Absorption Factor (F_v)

The inelastic energy absorption factor (F_v) accounts for the fact that an earthquake represents a limited energy source and many structures are capable of absorbing substantial amounts of energy beyond yield without loss of function. The parameter commonly used to measure the energy absorption capacity in the inelastic range is the system ductility, μ_{sys} . It is defined as the ratio of the summation of the product of each story weight and median displacement at ultimate capacity to the summation of the product of each story weight and story displacement at yielding of the critical story as shown below (Ref. 15-1):

$$\mu_{\text{sys}} = \frac{\sum W_i \cdot \delta_{Ti}}{\sum W_i \cdot \delta_{ei}} \quad (15.3-12)$$

Where:

W_i = weight of each story

δ_{Ti} = median maximum deflection of each story at ultimate capacity

δ_{ei} = median elastic deflection of each story scaled to reach yield in the critical story

A story drift of 0.5% is used to estimate the deflection profile at failure of the governing shear wall. Once the median system ductility is calculated, the median inelastic energy absorption factor is calculated using two different procedures, i.e., the Effective Frequency/Effective Damping Method and the Effective Riddell-Newmark Method (Ref. 15-1) and the average value is the median inelastic energy absorption factor of the structure.

A median damping value of 7% of critical is conservatively assumed in the inelastic energy absorption factor calculation. This is to avoid double-counting of energy dissipation due to hysteresis damping and inelastic response of the building.

The inelastic energy absorption factor of the Reactor Building shear wall is calculated to be 1.8. The associated randomness and uncertainty logarithmic standard deviations are 0.05 and 0.09, respectively determined from using the lower bound story drift of 0.36% (Table 3-5 of Ref. 15-1).

15.3.3.1.2 Structural Response Factor (F_{rs})

The structural response factor (F_{rs}) consists of a number of factors or parameters introduced in the calculation of structural response in the seismic dynamic analysis. Response calculations performed in the design analysis utilized conservative deterministic parameters. The actual response may differ significantly from the calculated response for a given peak ground acceleration level since many of these parameters are random. The structural response factor is evaluated as the product of the following factors that are considered to have the most influence on the structural response.

$$F_{rs} = F_{gm}F_dF_{ssi}F_mF_{mc}F_{ecc} \quad (15.3-13)$$

Where:

F_{gm} = ground motion factor accounting for the margin of the single envelope design ground response spectra with respect to the performance based seismic design spectra (Ref. 15-11) and conservative or unconservative bias in the treatment of horizontal direction peak response and vertical component response.

F_d = damping factor accounting for the variability in response due to difference in expected damping at failure and damping used in the analysis,

F_{ssi} = soil-structure interaction factor accounting for the variability associated with SSI effects on structural response,

- F_m = structural modeling factor accounting for the variability in response due to modeling assumptions,
- F_{mc} = modal response combination factor accounting for the variability in response due to the method used in combining modal responses,
- F_{ecc} = earthquake component combination factor accounting for the variability in response due to the method used in combining the earthquake components.

- Ground Motion Factor (F_{gm})

Three factors are considered under the ground motion factor, i.e., Spectral Shape Factor (F_{sa}), Horizontal Direction Peak Response (F_{HD}), and Vertical Component Response (F_V) as presented in this section.

- Spectral Shape Factor (F_{sa})

The ground response spectrum considered in the seismic design is the envelope of the 0.3g Regulatory Guide (RG) 1.60 site-independent ground spectra and the 0.5g North Anna ESP site-specific performance-based design ground spectra. The resulting single envelope design spectra are anchored to 0.5g peak ground acceleration as shown in Figure 15-2. The ground response spectrum used for the seismic margin assessment is also shown in Figure 15-2. In the frequency range lower than 9 Hz, a performance-based seismic design horizontal spectrum that bounds all the soil sites except Vogtle in the recent EPRI study (Ref. 15-15) is developed. This is due to the fact that the Reg. Guide 1.60 spectra which dominate in the frequency range below 9 Hz are more like 84th percentile spectra or higher. The envelope of this spectrum and the North Anna ESP performance-based design spectrum, hereafter called performance-based seismic design spectrum, is used for the seismic fragility calculation.

In accordance with the soil-structure interaction analysis performed and described in DCD Tier 2 Appendix 3A, generic medium soil stiffness sites yield the highest seismic responses. Therefore, the spectral shape factor is derived by comparing the single envelope design spectra with the performance-based seismic design spectra (see Figure 15-2) at the dominant frequency of the soil-structure system of medium soil stiffness site. The differences between these two spectra are the margins in the ground motion input. At the dominant frequency of 2.6 Hz of the reactor building in medium soil stiffness site, the 5% damped spectral accelerations of the two spectra are 0.93g and 0.59g, respectively. Thus the spectral shape factor is:

$$F_{sa} = 0.93g / 0.59g = 1.58 \quad (15.3-14)$$

Similarly a spectral shape factor of 1.37 is calculated for soft soil stiffness site. In consideration that soil stiffness is likely to degrade at the acceleration level where building failure is expected, an average value of 1.47 is used for the spectral shape factor.

The logarithmic standard deviation of randomness in the spectral shape factor is the peak to valley variability of the performance-based seismic design spectra, which is 0.2 according to Ref. 15-1. Since the Uniform Hazard Spectra (UHS) is derived from the probabilistic seismic hazard assessment, no uncertainty is assigned to the spectral shape factor to avoid double counting the uncertainty in the seismic hazard analysis.

- Horizontal Direction Peak Response (F_{HD})

The ground motion parameter (e.g., peak ground acceleration) is the average of the two horizontal directions. Thus, the ground motion in one direction may be higher than that in the perpendicular direction. For a box-type structure such as the Reactor Building, seismic demand of a major shear wall is affected primarily by one directional horizontal response. The effect of earthquake in the perpendicular direction is insignificant. Since an average parameter is used, the real response could be either higher or lower, hence no bias either way. Thus,

$$F_{HD} = 1.0 \quad (15.3-15)$$

The associated randomness and uncertainty are 0.13 and 0, respectively per Ref. 15-1.

- Vertical Component Response (F_V)

The vertical component of the ESBWR single envelope design spectra follows the Reg. Guide 1.60 vertical spectrum from 0.1 Hz up to 10 Hz and follows the North Anna performance-based design spectra above 10 Hz. This is conservative in comparison to the case where vertical component ground motion is assumed to be 2/3 of the horizontal component. Though relatively large randomness and uncertainty variability are associated with the vertical component (Table 3-2 of Ref. 15-1), because of the small effect the vertical component has on the governing failure mode of the building (i.e., shear wall failure), they are significantly diminished in the final fragility parameters. Therefore,

$$F_V = 1 \quad (15.3-16)$$

The associated randomness logarithmic standard deviation is 0.10. Therefore, the overall ground motion factor of safety is 1.47 ($= 1.47 * 1.0 * 1.0$) and the overall randomness is 0.26 by combining the randomness of spectral shape, horizontal direction peak response, and vertical component response per Equation 15.3-7.

- Damping Factor (F_d)

For reinforced concrete structures the damping ratio considered in the SSE analysis is 7%. The realistic values when the stress is at or near yield range from 7 to 10% (Ref. 15-14). The upper bound value is considered to be the median and the lower bound corresponds to the 84th percentile level.

Soil springs and dashpots are used in the soil-structure interaction modeling of the reactor building on generic sites. In such a soil-structure interaction system, the damping value of the building structure has less significant effect on the overall response of the building since soil modes are dominant. Thus, a factor of safety of unity is assigned to the damping factor.

$$F_d = 1 \quad (15.3-17)$$

The associated logarithmic standard deviation can be estimated using the ratio of the amplification factor at 84th percentile damping (AF_{bd}) to the amplification factor at median damping (AF_{md})

$$\beta_c = \ln (AF_{bd} / AF_{md}) \quad (15.3-18)$$

Since conservatism in the structure hysteretic damping of the design seismic response analysis is neglected above, no value is assigned to the uncertainty logarithmic standard deviation.

- Soil-Structure Interaction Factor (F_{SSI})

The factor of safety of soil-structure interaction between the reactor building and the supporting media includes the following considerations

- Ground motion incoherence (F_{GMI})
- Vertical spatial variation of ground motion (F_{VSV})
- SSI analysis (F_{SSI})

The dominant frequency of the SSI system of reactor building founded on uniform half space of medium soil stiffness site is 2.6 Hz. At this frequency the ground motion incoherence effects is insignificant, therefore, $F_{GMI} = 1.0$ and there is no variability associated with it.

The vertical spatial variation factor is to account for conservative bias in the SSI analysis that arises from choice of location of the control motion. The ground motion at the surface level in the free field decreases with depth of embedment. The ESBWR single envelope design ground spectra are defined as the outcrop motion at the foundation level of the reactor building for all site conditions. This conservative bias may be quantified if the surface ground motion is deconvoluted from the finished grade to the foundation level. Due to lack of this information, the embedment effect is estimated by using the design floor response spectra at the reactor building basemat for the medium soil site condition and the layered site condition. For the layered site cases, the surface motion calculated from SHAKE (SHAKE - the Free-Field Site Response Analysis, see DCD Appendix 3C.7.3 for program description) is used as input for the SASSI (SASSI - Dynamic Soil-Structure Interaction Analysis Program, for detail, see DCD Appendix 3C.7.2) calculation. The factor of safety due to embedment effect is determined to be 1.22. No reduction due to embedment is estimated at three standard deviations from the median case. Based on this the associated uncertainty variability is calculated to be 0.07. The randomness variability is estimated to be 0.08 per Ref. 15-1.

Furthermore, the median strength factor calculated in Section 15.3.3.1.1 is based on seismic demand of the medium soil site conditions. It is expected that soil degradation will occur at the ground acceleration level where the reactor building failure is calculated. It is observed from Appendix 3A of DCD Tier 2 that seismic responses of the soft soil site are lower than that of medium soil site. Therefore, the third factor of safety under the soil-structure interaction factor is to account for this effect and a factor of safety of 1.31 is calculated using the average responses of medium soil and soft soil site conditions.

The final SSI factor of safety is 1.6 ($= 1.22 \cdot 1.0 \cdot 1.31$) and the associated randomness and uncertainty variability are 0.08 and 0.28, respectively.

- Modeling Factor (F_m)

The reactor building structural model considered in the seismic design analysis is a multi-degree-of-freedom system constructed according to common modeling techniques and the Standard Review Plan (SRP) requirements in terms of number of degrees of freedom and subsystem decoupling. The model is thus considered to be best estimate and the resulting dynamic characteristics to be median-centered. The modeling factor is thus unity. Uncertainty in the modeling has effects on the mode shapes and modal frequencies of the structure. For soil sites, frequency uncertainty of the soil-structure system is primarily due to uncertainty in soil

properties and soil degradation at higher strain levels. Such uncertainty is estimated in the soil-structure interaction factor of safety. Thus, no uncertainty in response due to frequency uncertainty is included. A logarithmic standard deviation of 0.15 is estimated to account for uncertainty in the mode shape per Reference 15-1.

- Modal Response Combination Factor (F_{mc})

The method used in the seismic response analysis is the time history method solved by direct integrations. The phasing between individual modal responses is known and the total response is the algebraic sum of all modes of interest. The maximum response is thus precise and the modal response combination factor (F_{mc}) is unity. The associated uncertainties are less than the uncertainties associated with the response spectrum method, in which the maximum modal responses are combined by the SRSS method. Therefore, a nominal value of 0.05 is assigned to the logarithmic standard deviation of randomness.

- Earthquake Component Combination Factor (F_{ecc})

The effects of multi-directional earthquake excitation on structural response depend on the geometry, dynamic response characteristics, and relative magnitudes of the two horizontal and the vertical earthquake components. The design method to combine the contributions from different earthquake components is SRSS or 100-40-40. Either method is considered to result in a median-centered response. The earthquake component combination factor is 1.0.

The reactor building walls are designed to resist in-plane loads. The walls mainly respond to the horizontal motion parallel to the walls. The vertical loads on the walls due to the vertical excitation are typically less significant in contributing to the total stresses and there is an equal probability of acting upward or downward. The earthquake component combination effect on the wall design is thus not significant and a small logarithmic standard deviation of 0.05 is estimated.

15.3.3.1.3 Fragility Results for Reactor Building Complex

The result of the fragility analysis for the identified reactor building failure mode is summarized in Table 15-2. The overall safety factor is the product of the individual factors. The total logarithmic standard deviation is the SRSS value of the individual logarithmic standard deviations. The seismic fragility, in terms of median ground acceleration, is the product of the overall factor and the SSE design ground acceleration of 0.5g. The HCLPF calculated in accordance with Equation 15.3-7a is presented at the bottom of the table.

15.3.3.2 RCCV and RPV Pedestal

Other major structures inside the reactor building are the reinforced concrete containment vessel (RCCV) and the Reactor Pressure Vessel (RPV) pedestal. The pedestal is part of the RCCV pressure boundary. Both the RCCV and the pedestal are reinforced concrete cylindrical structures interconnected to the reactor building via walls and slabs which respond to the seismic input motion as an integral unit.

The governing failure mode of the RCCV is shear failure of the cylindrical wall below the RCCV. The critical location is determined by calculating the ratio of capacity to demand at different locations of the containment wall. This cylindrical wall is not part of the RCCV

pressure boundary, but it is on the seismic load path of the RCCV. The median shear capacity of the cylindrical wall is based on the equations in Appendix N of Ref. 15-2 that are developed from a considerable amount of testing conducted in Japan on scale models of reinforced and prestressed concrete containment structures. The equation is as shown below:

$$v_u = 0.8\sqrt{f_{c_m}} + \rho\sigma_y \leq 21.1\sqrt{f_{c_m}} \quad (15.3-19)$$

Where f_{c_m} is the median compressive strength of concrete of the containment wall (psi)

σ_y is the median yield strength of containment wall reinforcing steel (psi)

ρ is the effective reinforcing steel ratio of the containment wall

The median shear capacity of the cylindrical wall is

$$V_u = \frac{v_u \cdot \pi \cdot D \cdot t_w}{\alpha} \quad (15.3-20)$$

Where D is mean diameter of the cylindrical wall

t_w is thickness of the containment wall

α is a factor to convert the cross section area into effective shear area

$$\begin{aligned} \alpha &= 2.0 \text{ if } \frac{M}{V \cdot D_0} \leq 0.5 \\ &= 0.667 \cdot \left(\frac{M}{V \cdot D_0} \right) + 1.67 \text{ if } 0.5 \leq \frac{M}{V \cdot D_0} \leq 1.25 \\ &= 2.5 \text{ otherwise} \end{aligned} \quad (15.3-21)$$

Where M and V are overturning moment and story shear at the section where median capacity is calculated.

The flexural strength of the cylindrical wall is found to have a higher factor of safety than that of shear. The other factors of safety are calculated similar to that of reactor building. The median seismic capacity of the RCCV is 5.41g peak ground acceleration (pga) with an associated combined logarithmic standard deviation of 0.48. The HCLPF capacity is 1.75g pga. The summary table of the RCCV fragility is presented in Table 15-3.

The RPV pedestal is a thick-walled cylinder based on its geometry. The governing failure mode is tangential shear near the base. Flexural failure does not govern. The formula used for calculating the median shear strength of the pedestal is developed based on test data as discussed in Ref. 15-16. The median seismic capacity of the RPV pedestal is 5.1g peak ground acceleration (pga) with an associated combined logarithmic standard deviation of 0.5. The HCLPF capacity is 1.59g pga. The summary table of RPV pedestal fragility is presented in Table 15-4.

15.3.3.3 RPV Support Brackets

The eight RPV support brackets are located at the junction of the RPV pedestal and the vent wall structure. The brackets are made of structural steel and they provide structural support to the RPV as well as the Reactor Shield Wall (RSW).

The structural integrity analysis of the RPV support bracket is documented in DCD Tier 2 Appendix 3G. The calculated stresses of normal, severe, extreme, abnormal, and abnormal extreme conditions of the RPV support brackets are presented in the appendix. The most severe case of stresses in the RPV brackets is identified in Table 3G.1-41 of Appendix 3G to be the vertical plate size 150 mm in compression. Anchorage of the brackets to the pedestal wall is found to have higher strength factor than the vertical plate of the bracket. It is noted that the vertical plates of the brackets are dimensioned such that plate buckling will not occur prior to yielding of the plate material. Therefore, median yield strength of the vertical plate material (i.e., A516 Grade 70) is used to calculate a median strength factor of 7.39. The inelastic energy absorption factor is unity since failure of the bracket is considered to be localized.

The maximum enveloping seismic forces acting on the support brackets are from seismic response of the fixed base model with in-fill concrete stiffness of vent wall (VW) and diaphragm floor (DF). The fundamental frequency of the RPV of the fixed base model is estimated at 12 Hz. At this frequency, there is no margin between the single envelope design spectra and the performance-based seismic design spectra (see Figure 15-2). Thus, the spectral shape factor of safety is unity. A ground motion incoherence factor of safety of 1.15 is calculated using the approach in Ref. 15-1. The median seismic capacity of the RPV support brackets is 4.24g pga with an associated combined logarithmic standard deviation of 0.33. The HCLPF capacity is 2.0g pga. The summary table of RPV support bracket fragility is presented in Table 15-5.

15.3.3.4 Control Building Structure

The control building is a rectangular shape reinforced concrete box type structure. Its seismic fragility is evaluated using the same procedure described above for the reactor building. The controlling mode of failure is found to be shear failure of walls. Table 15-6 presents the margin in each of the capacity and response factors. The resulting median seismic capacity is 3.72 g pga with a logarithmic standard deviation of 0.51. The HCLPF capacity of the control building is 1.17g.

15.3.4 Component Fragility

The overall approach for determining HCLPF capacities of equipment and components qualified by seismic testing and analysis is described in EPRI TR-103959 (Ref. 15-1). Since the detailed design information on the equipment is not available at this time, generic HCLPF capacities of 1.67*SSE are assigned. These generic HCLPF capacities assumed for equipment and components are considered achievable because of the margins or safety factors introduced at different stages of equipment design and qualification. Equipment qualified for application in GE ESBWR plants has additional seismic margins in high frequencies due to design consideration of high-frequency hydrodynamic loads in combination with seismic loads. The other sources of margin are from conservatism in the ESBWR seismic response analysis, e.g., use of single enveloping design spectra and conservative treatment of soil-structure interaction and the use of enveloping responses of all site conditions for design.

The equipment and components of the GE ESBWR plant will be qualified to the required floor response spectra arising from the single envelope ground motion input rich in both low and high frequencies and following the ASCE, ASME and IPEEE Standards, their seismic HCLPF capacities should be able to meet the required value of 1.67 times 0.5g peak ground acceleration.

Given the single enveloping design spectra of ESBWR and the performance-based seismic design spectra, it becomes obvious that the rock sites will be most challenging to meet the required HCLPF capacity if the building frequency is higher than 9 Hz. At 9 Hz and above, the single enveloping design spectra is the same as the performance-based seismic design spectra such that the structural response factor will only be slightly greater than unity when other variables that would affect seismic response of the structures are considered. In such a case, the Required Response Spectra (RRS) will be appropriately factored throughout the frequency range to assure that the HCLPF margin of 1.67 will be met.

15.3.5 Fragility Summary

The structural seismic fragilities and corresponding HCLPF values of the Reactor Building, the RCCV, the RPV pedestal, the RPV support brackets, and the Control Building are summarized in Table 15-1. All have HCLPF seismic capacities greater than 1.67 times the SSE.

15.4 ACCIDENT SEQUENCE HCLPF ANALYSIS

An event tree structure is used in the ESBWR seismic margin analyses to illustrate the accident sequences analyzed in the analysis. This event tree structure is shown in Figure 15-3a and Figure 15-3b.

The seismic event tree is used to identify those structures and components requiring seismic capacity analysis (refer to Section 15.3), and to identify the HCLPFs of individual seismic-induced accident sequences.

If a system, S, (or sequence) contains two components (A, B) combined with OR logic, the failure of any component will fail the system ($S = A + B$), and the cumulative fragility distribution of the system is governed by the fragility distribution of the weakest component. This principle is applied to the system fault trees, which generally are comprised of OR gates.

If two elements operate in AND logic, only the failure of both components will fail the system ($S = A * B$), and the cumulative fragility distribution of the system is governed by the fragility distribution of the most seismically rugged component. This principle is applied to accident sequences, which are composed of AND elements.

The scope of this analysis includes both at-power and shutdown seismic-induced accident scenarios. The seismic accident analysis for the at-power condition is discussed below in Section 15.4.1, and the analysis for the shutdown condition is discussed in Section 15.4.2.

15.4.1 Full Power Analysis

15.4.1.1 Full Power Seismic Event Tree

The seismic event tree is shown in Figure 15-3a and Figure 15-3b. The HCLPF fragility information input into each event tree node is obtained from the fragility analysis summarized in Section 15.3. The HCLPF inputs as a function of event tree node are summarized in Table 15-7.

The event tree begins with the spectrum of seismic events, considers whether or not seismic-induced structural failure (node SI) occurs, and whether or not emergency DC power is lost. For seismic induced break outside containment in RWCU line, as shown in Figure 15-3b, a node for isolation of the RWCU line is added before the DC node to account for manual valve isolation. Loss of either structural integrity or DC power results in core damage. Thus, all remaining accident sequences in Figure 15-3a and Figure 15-3b are for cases of no structural failure and DC power available.

The success or failure of emergency DC power (node DC) is evaluated in Figure 15-3a and Figure 15-3b to account for support system dependencies. Failure of all DC power results in a high-pressure core melt since all control is lost, the isolation condensers fail, and the reactor cannot be depressurized.

In event of successful emergency DC, the next node questions whether or not seismic-induced failure to scram (node SCRAM) occurs. In the event of an ATWS, sufficient safety relief valves must open to prevent RPV failure due to overpressure. Failure of a sufficient number of safety relief valves to open is assumed to lead to a core damage condition due to the severe potential impact on boron injection effectiveness.

If the SRVs function properly, the next node questions the actuation of the Standby Liquid Control (SLCS) system. Seismic-induced failure of SLCS leads to a core damage condition.

For sequences with failure to scram (SCRAM node failure) but successful SLCS initiation, once the reactor is subcritical and all SRVs are closed, heat removal is achieved through the Isolation Condensers. No credit is given to the actuation of the Passive Containment Cooling system because of the impact on boron injection effectiveness. Failure of the Isolation Condenser after SLCS leads to a core damage condition.

To extend Isolation Condensers performance well beyond 24 hours, communication between the isolation condenser pools and the PCCS pools must be established. As an alternative to this action, water from a fire protection diesel driven pump may be aligned.

The successful condition of the Scram function (SCRAM node success) leads to another group of sequences. In this group, actuation of the SRVs is also required for initial pressure control. Additional RPV depressurization using the DPVs is required to allow low pressure injection. These valves discharge to the drywell and after their actuation, the Gravity Driven Cooling system (GDCS) is required to provide water to keep the core covered and to compensate for the water losses due to steam discharge to the drywell. Failure of either function will lead to core damage.

Heat removal from the drywell will be achieved through the actuation of the Passive Containment Cooling system (PCCS), a fully passive system that condenses the steam and drives the water back to the GDCS pools. In order to ensure that non-condensable gases cannot prevent steam circulation through PCCS heat exchangers it is necessary that the non-condensables be directed to the wetwell. In order to facilitate this process, wetwell pressure must be lower than drywell pressure. All vacuum breakers that separate the drywell from the wetwell must all be closed to prevent equalizing the wetwell and drywell pressure. It is considered that the failure of one vacuum breaker would prevent the successful operation of the PCCS and consequently would lead to core damage.

Whether heat removal is initially provided by either the isolation condensers (ATWS sequences) or the Passive Containment Cooling System (non-ATWS sequences), long term heat removal success requires that the isolation condensers pool be communicated with the PCCS pools. As an alternative to this action, water from a fire protection diesel driven pump may be aligned.

15.4.1.2 System Analysis

The seismic fault trees contain only those components that might be subject to seismic failure. One of the important ground rules of the seismic margin analysis is that all like components in a system always fail together.

The passive safety systems credited in the analysis have just a few active components (valves), all with automatic actuation and none with reliance on human action that might represent a single failure dominating the overall system reliability. Human actions are required only in the long term and as such, given the low likelihood of failure for operator actions with very long allowable time windows, human action errors do not dominate system failure. As such, random failures are assumed to be non-significant contributors to seismic risk (consistent with past industry seismic studies) and are not explicitly included in the analysis.

Structure failures judged to contribute to seismic core damage are shown on Figure 15-4. In this analysis, any one or more of these structural failures are assumed to result in core damage. The structures having the lowest seismic capacity are the reactor building and control building.

Most of the systems credited in the event tree are passive systems. The passive concept means that these systems do not require AC power supply for their actuation. However, DC power supply is required for a number of functions in those systems. The PCCS system is the only fully passive system. These systems require that depressurization valves actuate as well as the Gravity Driven System, and these systems have dependency on DC power. As such, the DC power supply is considered separately in the seismic event tree. The most critical components in the DC system are the batteries and cable trays that distribute cables associated with DC distribution. Motor control centers are also included, representing the panels that distribute DC and vital AC power to different loads. The seismic fault tree for DC power is shown on Figure 15-5.

The reactor protection system, control rod drive system, and alternate rod insertion system are not modeled because the failure of control rods to insert is dominated by the relatively low seismic fragility of the fuel assemblies, control rod guide tubes, and housings. The seismic fault tree for reactivity control is shown on Figure 15-6. The fuel assemblies are the most fragile component.

The seismic fault tree for safety relief valves, Figure 15-7, models the possible failures of the SRVs themselves. The seismic fault tree for the standby liquid control system is shown on Figure 15-8.

The seismic fault tree for the isolation condensers is shown in Figure 15-9. Heat exchanger failure is the most significant seismic-induced component failure, failures of nitrogen operated and motor operated valves and the piping are also included.

The seismic fault tree for the depressurization valves, Figure 15-10, models the possible failures of the DPVs themselves.

The gravity driven cooling system is a passive system and the seismic fault tree for this system, Figure 15-11, includes the failure of the squib and check valves, as well as the piping.

The seismic fault tree for the vacuum breakers, Figure 15-12, models the possible failures of the vacuum breakers themselves.

The passive containment cooling system is a fully passive system with no active components. The seismic fault tree for PCCS is shown in Figure 15-13; it includes failure of heat exchangers and failure of piping.

Communication between the upper pools requires only the opening of valves. The seismic fault tree for this function is shown in Figure 15-14.

The firewater diesel-driven pump is designed to supply water to the upper pools. The seismic fault tree for this function is shown in Figure 15-15.

For a LOCA event, a seismically induced break outside containment (BOC) in the RWCU line is shown in Figure 15-3b. Though seismically qualified, the inclusion of the RWCU system break outside containment presents a seismic margin capacity insight, especially given the significant

CDF contribution of the BOC in RWCU line among the LOCA events. The seismic fault tree for this function is shown in Figure 15-20.

The insight of a loss of preferred power event is included in the shutdown seismically induced event, as shown in Figure 15-17a.

15.4.2 Shutdown Analysis

The seismic shutdown analysis uses the same seismic margins approach, as well as many of the risk model elements used in the full power seismic analysis.

The HCLPF nodal fault trees used for the shutdown seismic analysis are the same as those used in the full power seismic analysis, with the exception of the structural failure node.

The seismic-induced initiating event assumed in the accident sequence analysis is Loss of Preferred Power (LOPP). Scenarios with structural failures are modeled as leading directly to core damage.

Three shutdown seismic event trees are developed to differentiate the major plant operation modes during shutdown conditions. The following three shutdown modes are addressed (consistent with the other external events shutdown analyses): Mode 5, Mode 6-Unflooded, and Mode 6-Flooded.

15.4.2.1 Shutdown Seismic Event Tree

The shutdown seismic fault tree and event trees are provided in Figures 15-16 through 15-19.

Mode 5 and Mode 5 Open

There are two modes modeled in Mode 5 in the shutdown risk analysis (Section 16), Mode 5 (cold shutdown) and Mode 5 Open (cold shutdown with containment open).

To address the specific time of concern in the shutdown risk analysis (Section 16), Mode 5 was divided into two, one being the Tech Spec defined Mode 5 and the other being called Mode 5 Open (Mode 5 with open containment).

The Mode 5 Open is not a Tech Spec defined Mode, and actually includes a period of time from two separate Tech Spec defined Modes. Mode 5 Open is essentially the same as Mode 5 with the exception being that there is no intact containment. The reactor vessel head is still on, but the containment is open.

Part of the Mode 5 Open period is actually part of the Tech Spec defined Mode 6. According to the Tech Spec mode definitions, Mode 6 begins when one or more reactor vessel head closure bolts is less than fully tensioned. Mode 5 Open sequences consider pressure relief in the model. Mode 6 sequences do not since the RPV head is removed for the majority of the mode. Due to the Tech Spec definition, there is a small period of time that is technically Mode 6, but where the vessel head may still provide a pressure seal. The period of Mode 6 with the vessel head still on is included in the Mode 5 Open shutdown risk analysis.

It is assumed in the shutdown risk analysis that the reactor vessel head on period in Mode 6 is bounded by the Mode 5 Open shutdown risk analysis.

The first node of the tree, SIS, models seismic-induced failures of the containment building, reactor building, control building, RPV pedestal or supports, fuel assemblies, CRD housing,

containment or shroud support. Failure of this node is modeled as leading directly to core damage.

The second node of the tree, DC, models seismic-induced failure of emergency DC power. As shown in Figure 15-5, this node models failure of the batteries, motor control centers or cable trays.

Success of the Isolation Condenser, represented by the IC node, guarantees short-term and long-term residual heat removal, even in the event of DC power failure. Failure of both IC and DC leads directly to core damage.

If the isolation condenser function fails but DC power is available, RPV pressure will increase and lead to the actuation of the safety valves, modeled by the SRV node. Sequences with success at the SRV node continue to the node representing fire protection system water injection into the RPV (FPW).

If the SRV function fails, RPV depressurization can be completed using the DPVs. Failure of both SRV and DPV leads directly to core damage.

Following successful RPV depressurization at the DPV node, actuation of the Gravity Driven Cooling System (GDCS node) is next challenged to supply water inventory to maintain the core covered and to compensate for water inventory losses due to steam discharge to the drywell.

For sequences in which the SRVs have failed but successful DPVs, the fire protection system (FPW) can be used as an alternative RPV injection method if GDCS fails.

There is no Tech Spec requirement of PCCS during shutdown condition, though the PCCS may be available for Mode 5 while containment is still intact. As shown in Table 15-10a, Table 15-10b, Figure 15-17a, and Figure 15-17b, for Seismic Margin Analysis, the seismic margin capacity insights would be the same for sequences whether PCCS was included in the event trees. (Table 15-10b and Figure 15-17b are for sensitivity to show insight).

Finally, the PI node models failure of the valve allowing communication between the upper pools.

Mode 6 (Unflooded)

The Mode 6-Unflooded shutdown seismic event tree is shown in Figure 15-18. As discussed previously, the event tree assumes a LOPP condition.

The two first nodes of the tree, SIS and DC, are the same as in the Mode 5 tree. Failure of either leads directly to core damage.

Long term cooling in this operation mode would be guaranteed by the actuation of the Fire Protection Water System modeled in the FPW node, or as an alternative, the Gravity Driven Cooling System (GDCS node).

Mode 6 (Flooded)

In this mode of operation, the cavity is flooded and the reactor vessel is open. If an earthquake occurred during this mode, no system would have to be actuated to guarantee long term cooling; only structural integrity would have to be maintained.

The Mode 6-Flooded shutdown seismic event tree, shown in Figure 15-19, includes only one node (SIS) that models maintaining structural integrity.

15.4.2.2 System Analysis

The HCLPF nodal fault trees used for the shutdown seismic analysis are the same as those used in the full power seismic analysis, with the exception of the structural failure node. The structural failure nodal fault tree (SIS), Figure 15-16, for the shutdown seismic event tree is developed to include the structural failures included in the full power SI nodal fault tree, as well as the structural elements related to reactivity control.

15.5 RESULTS

The results of the SMA HCLPF accident sequence analysis are shown on Figures 15-3, 15-17, 15-18 and 15-19, and in Tables 15-9, 15-10a and 15-10b. As can be seen, no accident sequence has a HCLPF lower than 0.84 g (i.e., 1.67 x SSE). As such, the ESBWR plant and equipment are shown to be capable of withstanding an earthquake with a magnitude at least 1.67 times the safe shutdown earthquake (SSE).

15.6 INSIGHTS

The ESBWR seismic margins HCLPF accident sequence analysis highlights the following key insights regarding the seismic capability of the ESBWR:

- (1) The ESBWR is inherently capable of safe shutdown in response to strong seismic events.
- (2) The most significant HCLPF sequences are seismic-induced loss of DC power and seismic-induced ATWS due to seismic-induced failure of the fuel channels and seismic-induced failure of the SLC tank (both with 0.84g HCLPF).

15.7 CONCLUSIONS

The ESBWR is inherently capable of safe shutdown in response to strong magnitude earthquakes beyond the design basis earthquake. The analysis shows that the ESBWR has a plant level HCLPF value of at least 1.67 times the Safe Shutdown Earthquake (SSE).

15.8 REFERENCES

- 15-1 Electric Power Research Institute, “Methodology for Developing Seismic Fragilities”, Prepared by J.W. Reed and R.P. Kennedy, EPRI TR-103959, June 1994.
- 15-2 Electric Power Research Institute, “A Methodology for Assessment of Nuclear Power Plant Seismic Margin”, EPRI NP-6041, June 1991.
- 15-3 ESBWR Design Control Document, 26A6642.
- 15-4 *PRA Procedures Guide*, NUREG/CR-2300, January 1983.
- 15-5 *Not Used*.
- 15-6 Harrison, S. W., Esfandiari, S., Pandya, D., and Ahmed, R., *Seismic Fragility Curves for Evaluation of Generic Electrical Conduit Supports, to be presented in the ASME PVP Annual Meetings*, Honolulu, Hawaii, July 22-24, 1989.
- 15-7 Campbell, R. D., Ravindra, M. K., and Bhatia, A., *Compilation of Fragility Information from Available Probabilistic Risk Assessments*, LLNL, September 1985.
- 15-8 *Report on Quantification of Uncertainties, Report of Seismic Analysis Main Committee*, ASCE, March 15 1983.
- 15-9 *Severe Accident Risk Assessment—Limerick Generating Station*, NUS Report, April 1983.
- 15-10 *Handbook of Nuclear Power Plant Seismic Fragilities, Seismic Safety Margins Research Program*, NUREG/CR-3558, June 1985.
- 15-11 ASCE/SEI 43-05, *Seismic Design Criteria for Structures, Systems, and Components in Nuclear Facilities*, American Society of Civil Engineers.
- 15-12 Kennedy, R. P., and Ravindra, M. K., *Seismic Fragilities for Nuclear Power Plant Risk Studies, Nuclear Engineering and Design*, PP47-68, (79) 1984.
- 15-13 *Structural Analysis and Design of Nuclear Plant Facilities, Manual and Reports on Engineering Practice*, No. 58, ASCE, 1980.
- 15-14 *Development of Criteria for Seismic Review of Selected Nuclear Power Plants*, NUREG/CR-0098, May 1978.
- 15-15 Electric Power Research Institute “Assessment of Performance-Based Approach for Determining the SSE Ground Motion for New Plant Sites, V 1: Performance-Based Seismic Design Spectra”, Product ID # 1012044, Final Report, June 2005.
- 15-16 Bader, M and H. Krawinkler, "Shear Transfer in Thick-Walled Reinforced Concrete Cylinders", 6th SMiRT, Paris, France, August 1981.
- 15-17 Design Control Document Tier 2, Section 3.7.1, Seismic Design Parameters.

Table 15-1
Seismic Capacity Summary

Structure/Component	Failure Mode	Fragility		HCLPF (g) ⁽³⁾
		Capacity ⁽¹⁾ A _m (g)	Combined ⁽²⁾ Uncertainty	
Reactor Building	Shear failure of wall	3.57	0.47	1.2
Containment	Shear	5.41	0.48	1.75
RPV Pedestal	Shear	5.1	0.5	1.59
RPV support brackets	Yielding of bracket	4.24	0.33	2.0
Control building	Shear	3.72	0.5	1.17

Notes to Table 15-1:

- (1) Capacities are in terms of median peak ground acceleration.
- (2) Combined uncertainties are composite logarithmic standard deviations of uncertainty and randomness.
- (3) HCLPF capacity for components that are significant contributors to overall plant level seismic margin is assumed to be 0.84g minimum which is 1.67 times SSE.

Table 15-2
Seismic Fragility for Reactor Building Shear Walls

Failure Mode:		Shear Failure of Wall Along Column Line R1			
Factor of Safety		Median Value	β_R	β_U	
F_C	F _S	Strength	1.82	0.00	0.20
	F	Inelastic Energy Absorption	1.66	0.04	0.04
F_{RS}	F _{SA}	Spectral Shape			
		<i>Response Spectrum Shape</i>	1.47	0.20	0.00
		<i>Horizontal Direction Peak Response</i>	1.00	0.13	0.00
		<i>Vertical Component Response</i>	1.00	0.10	0.00
	F _D	Damping	1.00	0.00	0.00
	F _M	Modeling	1.00	0.00	0.15
	F _{MC}	Modal Response Combination	1.00	0.05	0.00
	F _{ECC}	Earthquake Component Combination	1.00	0.05	0.00
	F _{SSI}	Soil Structure Interaction			
		<i>Ground Motion Incoherence</i>	1.00	0.00	0.00
		<i>Vertical Spatial Variation</i>	1.22	0.08	0.07
	<i>SSI Analysis</i>	1.37	0.00	0.27	
Overall Factor of Safety			7.13	0.28	0.38
A _d = Peak Ground Acceleration of the Single Envelope Design Spectra = 0.5g					
A _m = Median Peak Ground Acceleration = F*A _d = 3.57g					
β _C = Combined Logarithmic Standard Deviation = 0.47					
HCLPF = 1.2g					

Table 15-3
Seismic Fragility for Containment Wall

Component:		Cylindrical Wall Below Reinforced Concrete Containment Vessel (RCCV)			
Failure Mode:		Shear			
Factor of Safety			Median Value	β_R	β_U
F_C	F_S	Strength	3.16	0.00	0.21
	F	Inelastic Energy Absorption	1.49	0.06	0.11
F_{RS}	F_{SA}	Spectral Shape			
		<i>Response Spectrum Shape</i>	1.47	0.20	0.00
		<i>Horizontal Direction Peak Response</i>	1.00	0.13	0.00
		<i>Vertical Component Response</i>	1.00	0.10	0.00
	F_D	Damping	1.00	0.00	0.00
	F_M	Modeling	1.00	0.00	0.15
	F_{MC}	Modal Response Combination	1.00	0.05	0.00
	F_{ECC}	Earthquake Component Combination	1.00	0.12	0.00
	F_{SSI}	Soil Structure Interaction			
		<i>Ground Motion Incoherence</i>	1.00	0.00	0.00
		<i>Vertical Spatial Variation</i>	1.22	0.08	0.07
	<i>SSI Analysis</i>	1.28	0.00	0.24	
Overall Factor of Safety			10.82	0.30	0.38
A_d = Peak Ground Acceleration of Single Envelope Design Spectra = 0.5g					
A_m = Median Peak Ground Acceleration = $F \cdot A_d$ = 5.41g					
β_C = Combined Logarithmic Standard Deviation = 0.48					
HCLPF = 1.75g					

Table 15-4
Seismic Fragility for RPV Pedestal

Component:		Reactor Pressure Vessel Pedestal			
Failure Mode:		Shear			
Factor of Safety			Median Value	β_R	β_U
F_C	F_S	Strength	3.29	0.00	0.25
	F	Inelastic Energy Absorption	1.34	0.06	0.10
F_{RS}	F_{SA}	Spectral Shape			
		<i>Response Spectrum Shape</i>	1.48	0.20	0.00
		<i>Horizontal Direction Peak Response</i>	1.00	0.13	0.00
		<i>Vertical Component Response</i>	1.00	0.10	0.00
	F_D	Damping	1.00	0.00	0.00
	F_M	Modeling	1.00	0.00	0.15
	F_{MC}	Modal Response Combination	1.00	0.05	0.00
	F_{ECC}	Earthquake Component Combination	1.00	0.12	0.00
	F_{SSI}	Soil Structure Interaction			
		<i>Ground Motion Incoherence</i>	1.00	0.00	0.00
		<i>Vertical Spatial Variation</i>	1.22	0.08	0.07
	<i>SSI Analysis</i>	1.28	0.00	0.24	
Overall Factor of Safety			10.19	0.30	0.40
A_d = Peak Ground Acceleration of Single Envelope Design Spectra = 0.5g					
A_m = Median Peak Ground Acceleration = $F \cdot A_d$ = 5.1g					
β_C = Combined Logarithmic Standard Deviation = 0.5					
HCLPF = 1.59g					

Table 15-5
Seismic Fragility for RPV Support Brackets

Component:		RPV Support Brackets			
Failure Mode:		Yielding of Vertical Plate of the Bracket			
Factor of Safety			Median Value	β_R	β_U
F_C	F_S	Strength	7.39	0.00	0.12
	F	Inelastic Energy Absorption	1.00	0.00	0.00
F_{RS}	F_{SA}	Spectral Shape			
		<i>Response Spectrum Shape</i>	1.00	0.20	0.00
		<i>Horizontal Direction Peak Response</i>	1.00	0.13	0.00
		<i>Vertical Component Response</i>	1.00	0.10	0.00
	F_D	Damping	1.00	0.00	0.00
	F_M	Modeling	1.00	0.00	0.13
	F_{MC}	Modal Response Combination	1.00	0.05	0.00
	F_{ECC}	Earthquake Component Combination	1.00	0.05	0.00
	F_{SSI}	Soil Structure Interaction			
		<i>Ground Motion Incoherence</i>	1.15	0.00	0.07
		<i>Vertical Spatial Variation</i>	1.00	0.00	0.00
	<i>SSI Analysis</i>	1.00	0.00	0.00	
Overall Factor of Safety			8.47	0.27	0.19
A_d = Peak Ground Acceleration of Single Envelope Design Spectra = 0.5g A_m = Median Peak Ground Acceleration = $F \cdot A_d = 4.24g$ β_C = Combined Logarithmic Standard Deviation = 0.33 HCLPF = 2.0g					

Table 15-6
Seismic Fragility for Control Building

Component:		Control Building			
Failure Mode:		Shear Failure of Wall Along Column Line CA			
Factor of Safety			Median Value	β_R	β_U
F_C	F_S	Strength	2.36	0.00	0.20
	F	Inelastic Energy Absorption	1.63	0.06	0.10
F_{RS}	F_{SA}	Spectral Shape			
		<i>Response Spectrum Shape</i>	1.42	0.20	0.00
		<i>Horizontal Direction Peak Response</i>	1.00	0.13	0.00
		<i>Vertical Component Response</i>	1.00	0.10	0.00
	F_D	Damping	1.00	0.00	0.00
	F_M	Modeling	1.00	0.00	0.15
	F_{MC}	Modal Response Combination	1.00	0.05	0.00
	F_{ECC}	Earthquake Component Combination	1.00	0.05	0.00
	F_{SSI}	Soil Structure Interaction			
		<i>Ground Motion Incoherence</i>	1.00	0.00	0.00
		<i>Vertical Spatial Variation</i>	1.00	0.00	0.00
	<i>SSI Analysis</i>	1.36	0.00	0.31	
Overall Factor of Safety			7.44	0.29	0.42
A_d = Peak Ground Acceleration of Single Design Spectra = 0.5g					
A_m = Median Peak Ground Acceleration = $F \cdot A_d$ = 3.72g					
β_C = Combined Logarithmic Standard Deviation = 0.5					
HCLPF = 1.17g					

Table 15-7
ESBWR Systems and Components/Structures Fragilities

System/Component as a function of Event Tree Node	A _m (g)	β _c	HCLPF(g)
<u>PLANT ESS STRUCTURES (SI)</u>			
- Reactor Building (FRBLDG) ⁽¹⁾	3.57	0.47	1.2
- Containment (FCONT)	5.41	0.48	1.75
- RPV Pedestal (FPEDST)	5.1	0.5	1.59
- Control Building (FCTRBLDG)	3.72	0.5	1.17
- Reactor Pressure Vessel Support (FRPV)	4.24	0.33	2.0
<u>DC POWER (DC)</u>			
- Batteries (FBTR)			0.84
- Cable trays (FCTRAY)			0.84
- Motor control centers (FMCC)			0.84
<u>REACTIVITY CONTROL SYSTEM (SCRAM)</u>			
- Fuel assembly (FFASSY)			0.84
- CRD Guide tubes (FCRDGTB)			0.84
- Shroud support (FSHRSP)			0.84
- CRD Housing (FCRDHS)			0.84
- Hydraulic control unit (FHYLTUT)			0.84
<u>SAFETY RELIEF VALVE (SRV)</u>			
- SRV (FSRV)			0.84
<u>STANDBY LIQUID CONTROL (SLCS)</u>			
- Accumulator Tank (FACCT)			0.84
- Check valve (FCHV)			0.84
- Squib valve (FSQUV)			0.84
- Piping (FPIP)			0.84
- Valve (air operated) (FAOV)			0.84
<u>ISOLATION CONDENSER (IC)</u>			
- Piping (FPIP)			0.84
- Heat exchanger (FICHEX)			0.84
- Valve (motor operated) (FMOV)			0.84

Table 15-7
ESBWR Systems and Components/Structures Fragilities

System/Component as a function of Event Tree Node	A_m(g)	β_c	HCLPF(g)
- Valve (nitrogen operated) (FNOV)			0.84
<u>DEPRESSURIZATION VALVE (DPV)</u>			
- DPV (FDPV)			0.84
<u>GRAVITY-DRIVEN COOLING (GDCCS)</u>			
- Check valve (FCHV)			0.84
- Squib valve (FSQUV)			0.84
- Piping (FPIP)			0.84
<u>VACUUM BREAKERS (VB)</u>			
- Vacuum breakers (FVBS)			0.84
<u>PASSIVE CONTAINMENT COOLING (PCCS)</u>			
- Heat Exchanger (FPCCSHEX)			0.84
- Piping (FPIP)			0.84
<u>IC/PCC POOL INTERCONNECTION (PI)</u>			
- Valve (motor operated) (FIC/PCCI)			0.84
<u>FIRE PROTECTION WATER SYSTEM (FPW)</u>			
Pump (diesel driven) (FPUMPDD)			0.84
- Tank (FTANK)			0.84
- Piping (FPIP)			0.84
- FWSC (FFWSC) ⁽²⁾			1.13

Notes to Table 15-7:

- (1) Variables are used in Table 15-8.
- (2) For the Fire Water Service Complex (FWSC), per Ref. 15-17, the FWSC Certified Seismic Design Response Spectra (CSDRS) is 1.35 times the Design CSDRS. As such, the minimum HCLPF for the FWSC is 1.67*1.35*SSE.

Table 15-8
Seismic Event Tree Nodal HCLPF Equations

Top Event	Nodal HCLPF Equations^{(1) (2)}
Structural Integrity (SI)	$FSTRUC = FRBLDG + FCONT + FPEDST + FCTRBLDG + FRPV = (1.2g + 1.75g + 1.59g + 1.17g + 2.0g) = 1.17g$
DC Power (DC)	$FDCP = FBTR + FCTRAY + FMCC = (0.84g + 0.84g + 0.84g) = 0.84g$
Scram (SCRAM)	$FRC = FFASSY + FCRDGTB + FSHRSPT + FCRDHS + FHYCTUT = (0.84g + 0.84g + 0.84g + 0.84g + 0.84g) = 0.84g$
SRVs (SRV)	$FSRV = FSRVS = 0.84g$
Standby Liquid Control (SLCS)	$FSLCS = FACCT + FCHV + FSQUV + FPIP + FAOV = (0.84g + 0.84g + 0.84g + 0.84g + 0.84g) = 0.84g$
Isolation Condensers (IC)	$FIC = FPIP + FICHEX + FMOV + FNOV = (0.84g + 0.84g + 0.84g + 0.84g) = 0.84g$
DPVs (DPV)	$FDPV = FDPVS = 0.84g$
Gravity Driven Cooling System (GDSCS)	$FGDCS = FCHV + FSQUV + FPIP = (0.84g + 0.84g + 0.84g) = 0.84g$
Vacuum Breakers (VB)	$FVB = FVBS = 0.84g$
Passive Containment Cooling (PCCS)	$FPCCS = FPCCSHEX + FPIP = (0.84g + 0.84g) = 0.84g$
IC/PCC Pool Interconnection (PI)	$FIC/PCCINT = PIC/PCCI = 0.84g$
Fire Protection Water (FPW)	$FFPW = FPUMPDD + FTANK + FPIP + FFWSC = (0.84g + 0.84g + 0.84g + 1.13g) = 0.84g$
Structural Integrity Shutdown (SIS)	$FSTRUCSH = FRBLDG + FCTRBLDG + FRPV + FFASSY + FPEDST + FSHRSPT + FCONT + FCRDHS = (1.2g + 1.17g + 2.0g + 0.84g + 1.59g + 0.84g + 1.75g + 0.84g) = 0.84g$

Notes to Table 15-8:

- (1) Refer to nodal fault trees (Figures 15-4 through 15-5) for descriptions of the individual fragility basic events.
- (2) Per the MIN-MAX convention used, the overall fragility of a group of inputs combined using OR logic is determined by the lowest fragility input.

Table 15-9
HCLPF Derivation for Figure 15-3a and Figure 15-3b
(MIN-MAX Method)

SET Sequence	Sequence HCLPF⁽¹⁾
<u>Figure 15-3a</u>	
Sequence 3	$PI*FPW = 0.84g*0.84g = 0.84g$
Sequence 4	$PCCS = 0.84g$
Sequence 5	$VB = 0.84g$
Sequence 6	$GDCS = 0.84g$
Sequence 7	$DPV = 0.84g$
Sequence 8	$SRV = 0.84g$
Sequence 11	$SCRAM*PI*FPW = 0.84g*0.84g*0.84g = 0.84g$
Sequence 12	$SCRAM*IC = 0.84g*0.84g = 0.84g$
Sequence 13	$SCRAM*SLCS = 0.84g*0.84g = 0.84g$
Sequence 14	$SCRAM*SRV = 0.84g*0.84g = 0.84g$
Sequence 15	$DC = 0.84g$
Sequence 16	$SI = 1.17g$
<u>Figure 15-3b</u>	
Sequence 16	$IRWCU = 0.84g$
Sequence 17	$SI = 1.17g$

Notes to Table 15-9:

- (1) Per the MIN-MAX convention used, the overall fragility of a group of inputs combined using AND logic is determined by the highest fragility input.

**Table 15-10a HCLPF Derivation for Figure 15-17a, Figure 15-18 and Figure 15-19
(MIN-MAX Method)**

MODE 5

SET Sequence	Sequence HCLPF(1)
Sequence 4	$IC * FPW * GDCS = 0.84g * 0.84g * 0.84g = 0.84g$
Sequence 5	$IC * FPW * DPV = 0.84g * 0.84g * 0.84g = 0.84g$
Sequence 8	$IC * FPW * GDCS * FPW = 0.84g * 0.84g * 0.84g * 0.84g = 0.84g$
Sequence 9	$IC * SRV * DPV = 0.84g * 0.84g * 0.84g = 0.84g$
Sequence 11	$DC * IC = 0.84g * 0.84g = 0.84g$
Sequence 12	$SIS = 0.84g$

MODE 6 UNFLOODED

SET Sequence	Sequence HCLPF(1)
Sequence 3	$FPW * GDCS = 0.84g * 0.84g = 0.84g$
Sequence 5	$DC * FPW = 0.84g * 0.84g = 0.84g$
Sequence 6	$SIS = 0.84g$

MODE 6 FLOODED

SET Sequence	Sequence HCLPF
Sequence 2	$SIS = 0.84g$

Notes to Table 15-10:

- (1) Per the MIN-MAX convention used, the overall fragility of a group of inputs combined using AND logic is determined by the highest fragility input.

**Table 15-10b HCLPF Derivation for
ESBWR Shutdown Seismic Event Tree Sequences For Figure 15-17b
(Sensitivity) (MIN-MAX Method)**

MODE 5

SET Sequence	Sequence HCLPF⁽¹⁾
Sequence 4	IC *FPW*PI = 0.84g *0.84g *0.84g = 0.84g
Sequence 5	IC *FPW*PCCS = 0.84g *0.84g *0.84g = 0.84g
Sequence 6	IC *FPW*VB = 0.84g *0.84g *0.84g = 0.84g
Sequence 7	IC *FPW*GDCS = 0.84g*0.84g*0.84g = 0.84g
Sequence 8	IC *FPW*DPV = 0.84g*0.84g *0.84g = 0.84g
Sequence 10	IC *SRV*PIT = 0.84g *0.84g*0.84g = 0.84g
Sequence 11	IC *SRV* PCCS = 0.84g*0.84g*0.84g = 0.84g
Sequence 12	IC *SRV* VB = 0.84g*0.84g*0.84g = 0.84g
Sequence 14	IC *SRV* GDCS*PIT = 0.84g*0.84g*0.84g*0.84g = 0.84g
Sequence 15	IC* SRV* GDCS* PCCS = 0.84g*0.84g*0.84g*0.84g = 0.84g
Sequence 16	IC *SRV* GDCS* VB = 0.84g*0.84g*0.84g*0.84g = 0.84g
Sequence 17	IC *SRV* GDCS* FPW = 0.84g*0.84g*0.84g*0.84g = 0.84g
Sequence 18	IC *SRV* DPV = 0.84g*0.84g*0.84g = 0.84g
Sequence 20	IC *DC = 0.84g*0.84g = 0.84g
Sequence 21	SIS = 0.84g

Notes to Table 15-10:

- (1) Per the MIN-MAX convention used, the overall fragility of a group of inputs combined using AND logic is determined by the highest fragility input.

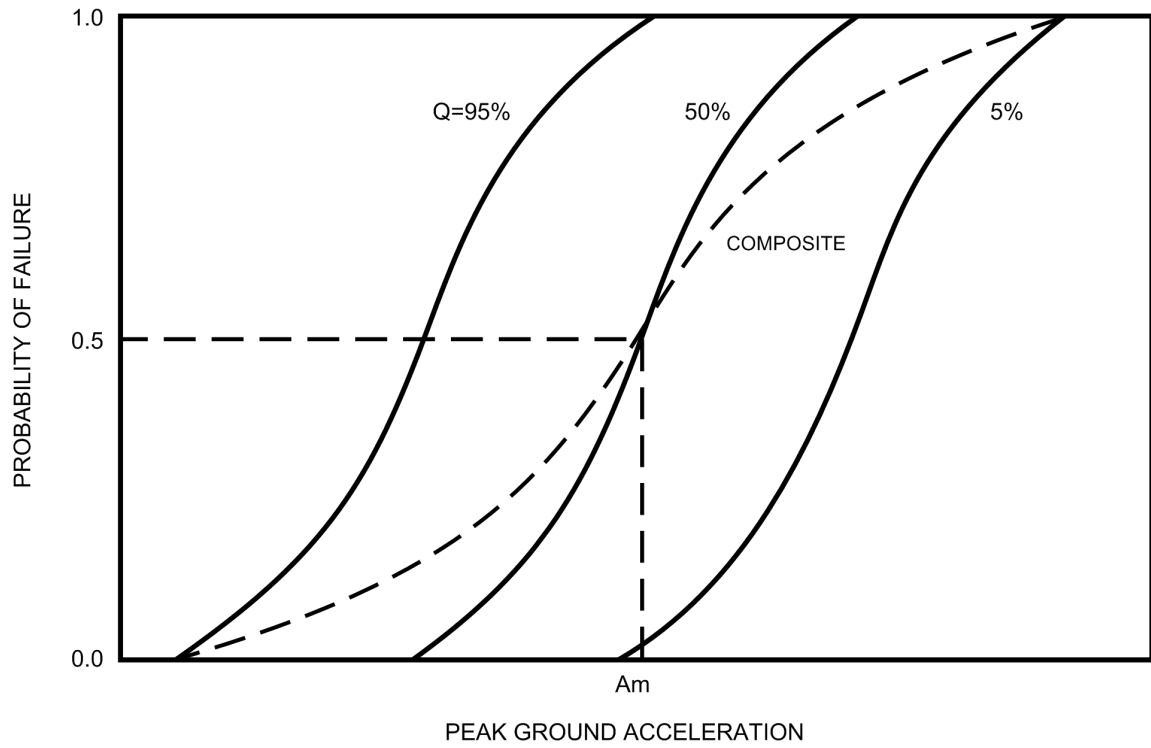


Figure 15-1. Typical Fragility Curves

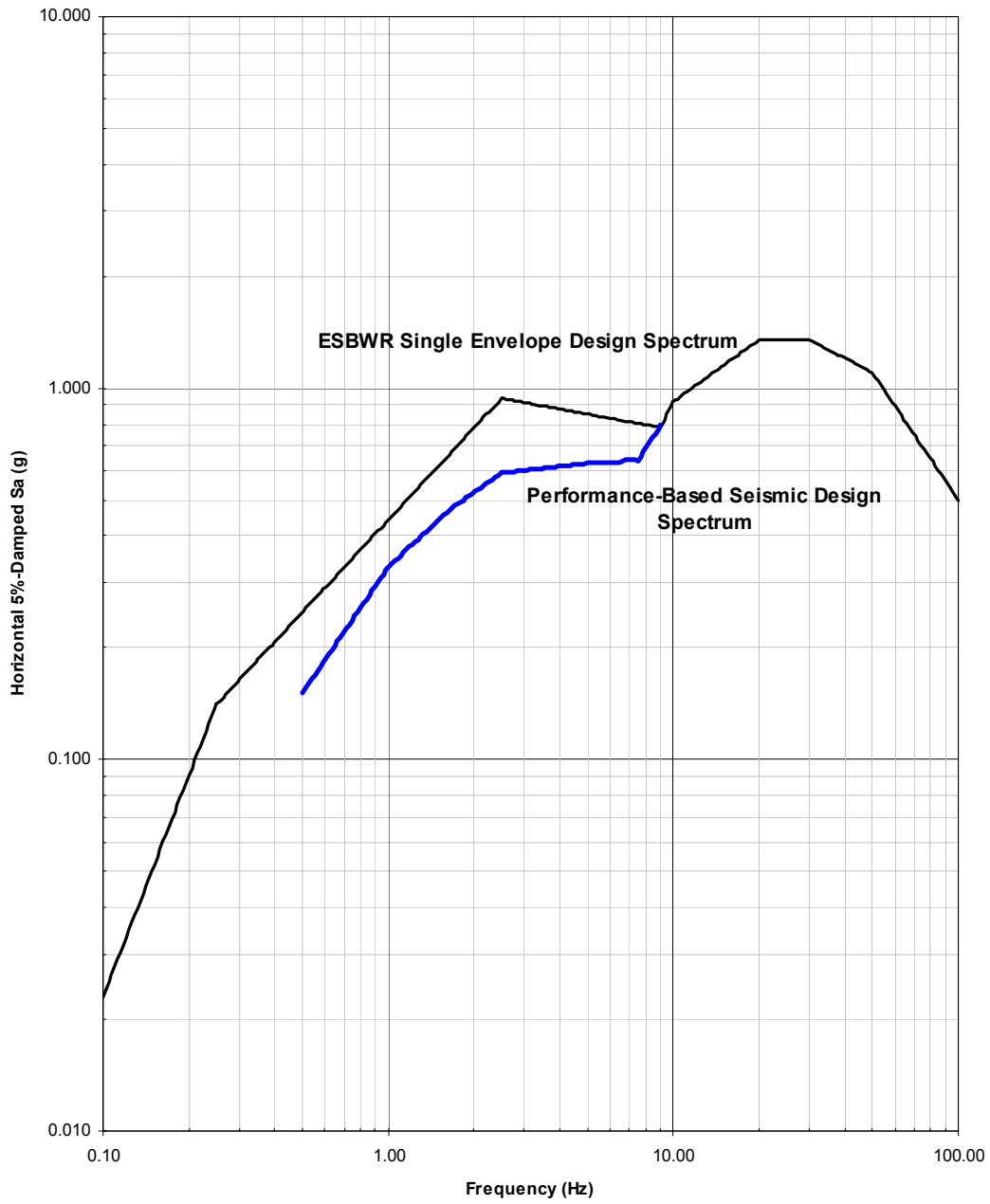


Figure 15-2. Horizontal Single Envelope Design and Performance-Based Seismic Design Spectra of ESBWR

SEISMIC EVENT	SI	DC	SCRAM	ADS/SRV	SLCS	IC	DPV	GDCS	VB	PCCS	PI	FPW	Number	Class	Min-Max
Seismic Event Full Power	STRUCTURAL INTEGRITY	DC POWER	SCRAM	ADS/SRV's	STANDBY LIQUID CONTROL	ISOLATION CONDENSER	DPV's	GRAVITY DRIVEN COOLING	VACUUM BREAKERS	PASIVE CONTAINMENT COOLING	IC/PCC POOL INTERCONNECTION	FIRE PROTECTION WATER			
													1		
													2		
													3	CD	0.84g
													4	CD	0.84g
													5	CD	0.84g
													6	CD	0.84g
													7	CD	0.84g
													8	CD	0.84g
													9		
													10		
													11	CD	0.84g
													12	CD	0.84g
													13	CD	0.84g
													14	CD	0.84g
													15	CD	0.84g
													16	CD	1.17g

Figure 15-3a. Seismic Event Tree (Full Power)

SEISMIC EVENT	SI	I RWCU	DC	SCRAM	ADS/SRV	SLCS	IC	DPV	GDCS	VB	PCCS	PI	FPW	Number	Class	Min-Max
Break Outside Containment in RWCU	STRUCTURAL INTEGRITY	Isolation of RWCU line	DC POWER	SCRAM	ADS/SRVs	STANDBY LIQUID CONTROL	ISOLATION CONDENSER	DPV's	GRAVITY DRIVEN COOLING	VACUUM BREAKERS	PASIVE CONTAINMENT COOLING	IC/PCC POOL INTERCONNECT ION	FIRE PROTECTION WATER			
<p>The diagram is a fault tree for the event 'Break Outside Containment in RWCU'. It starts with a top event labeled '%BOC-RWCU' at the bottom left. From this event, several branches lead to intermediate events: 'FSTRUC', 'FISORWCU', 'FDCP', 'FRC', 'FSRV', 'FSLCS', 'FIC', 'FDPV', 'FGDCS', 'FVB', 'FPCCS', 'FPIC/PCCI', and 'FFPW'. These intermediate events then lead to a final set of 17 numbered events (1-17) on the right side of the table. The 'Number' column lists these events, the 'Class' column lists 'CD' for all, and the 'Min-Max' column lists '0.84g' for events 1-16 and '1.17g' for event 17.</p>														1		
														2		
														3	CD	0.84g
														4	CD	0.84g
														5	CD	0.84g
														6	CD	0.84g
														7	CD	0.84g
														8	CD	0.84g
														9		
														10		
														11	CD	0.84g
														12	CD	0.84g
														13	CD	0.84g
														14	CD	0.84g
														15	CD	0.84g
														16	CD	0.84g
														17	CD	1.17g

Figure 15-3b. Seismic Induced Break Outside Containment in RWCU Line (Full Power)

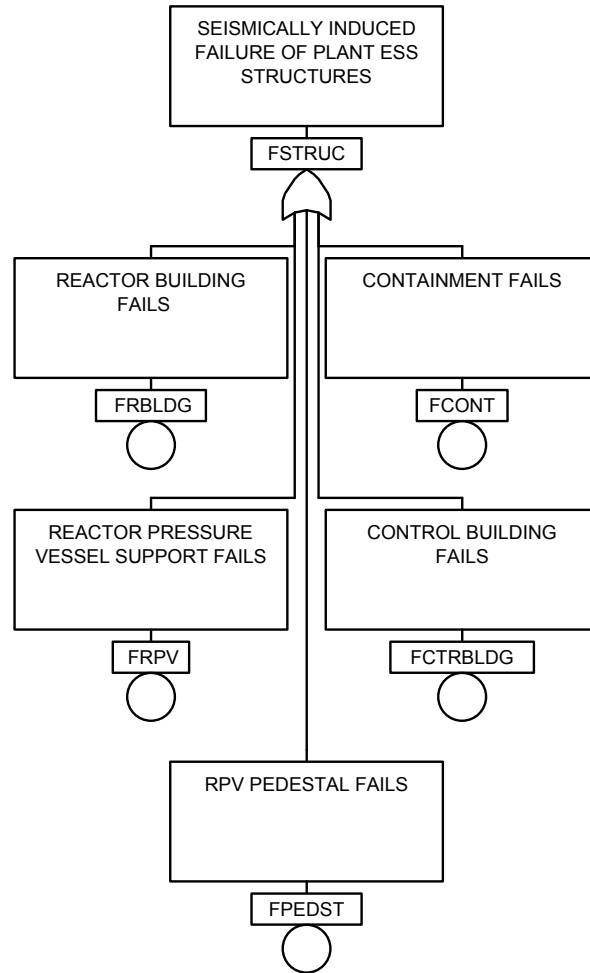


Figure 15-4. Structural Seismic Fault Tree (Full Power)

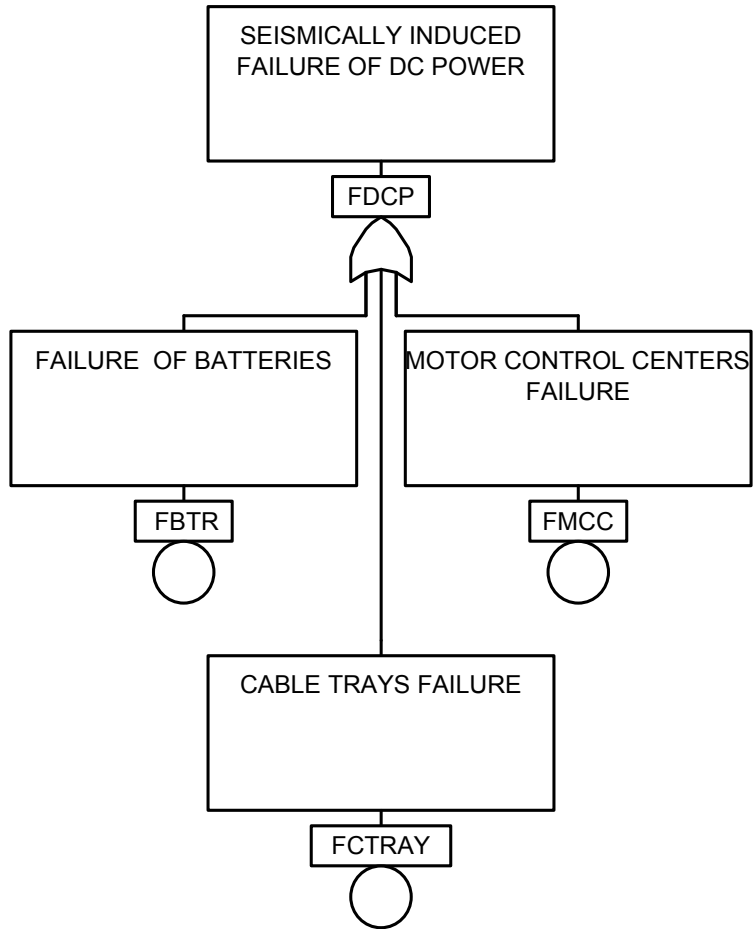


Figure 15-5. DC Power Seismic Fault Tree

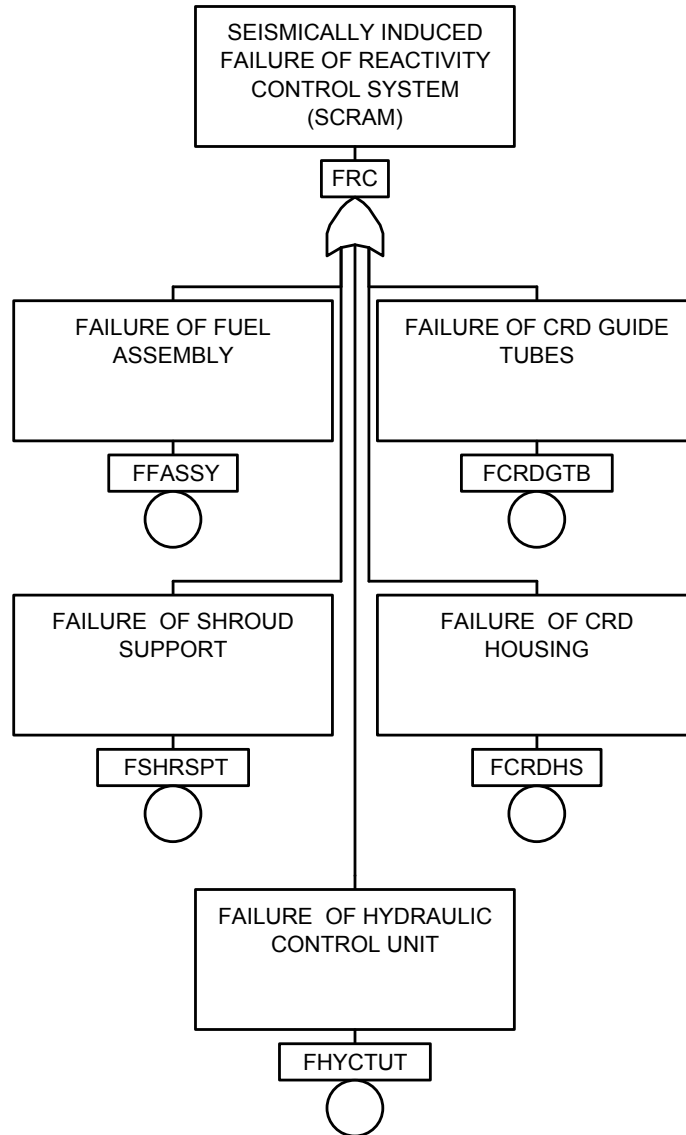


Figure 15-6. SCRAM Seismic Fault Tree

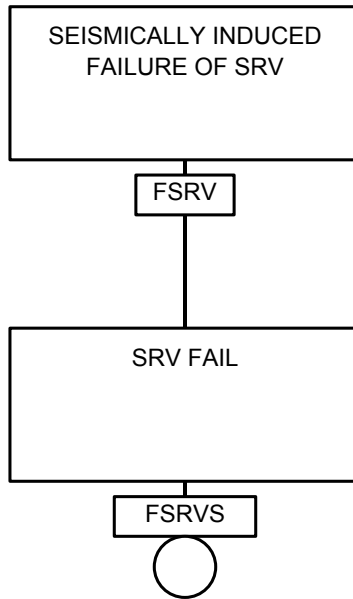


Figure 15-7. SRV Seismic Fault Tree

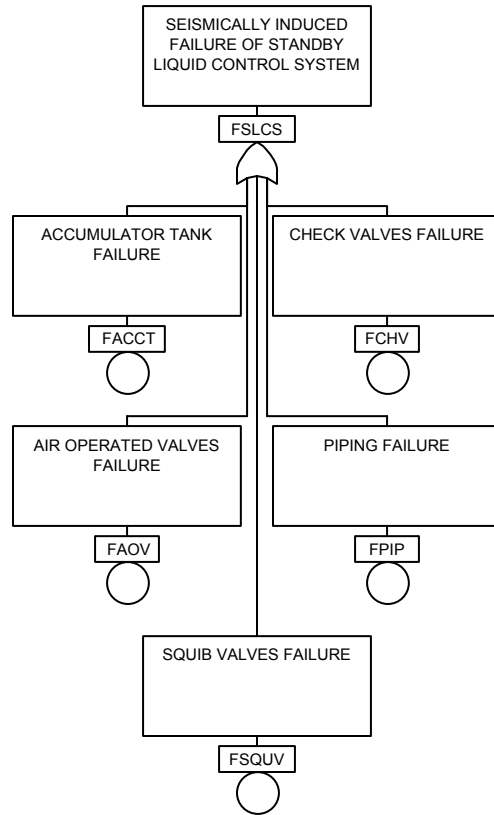


Figure 15-8. SLCS Seismic Fault Tree

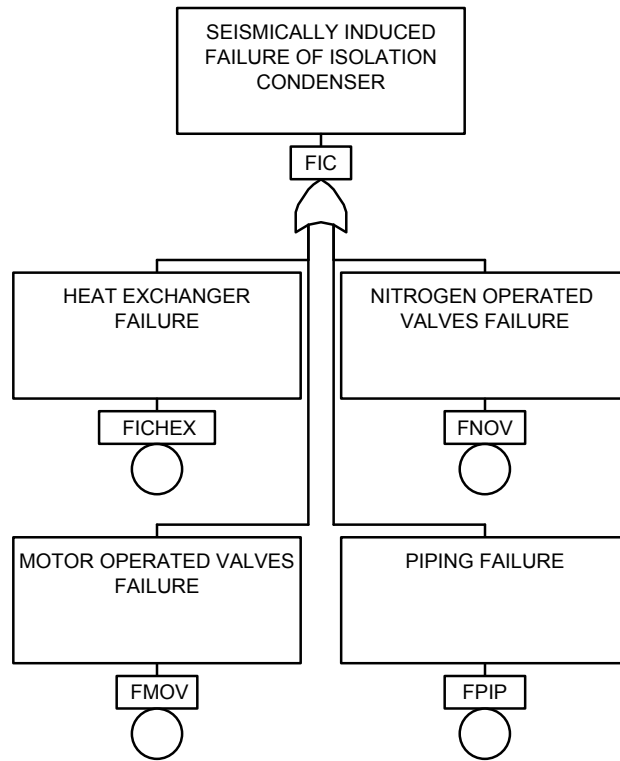


Figure 15-9. IC Seismic Fault Tree

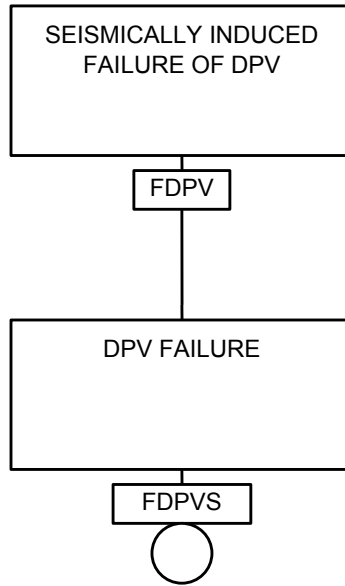


Figure 15-10. DPV Seismic Fault Tree

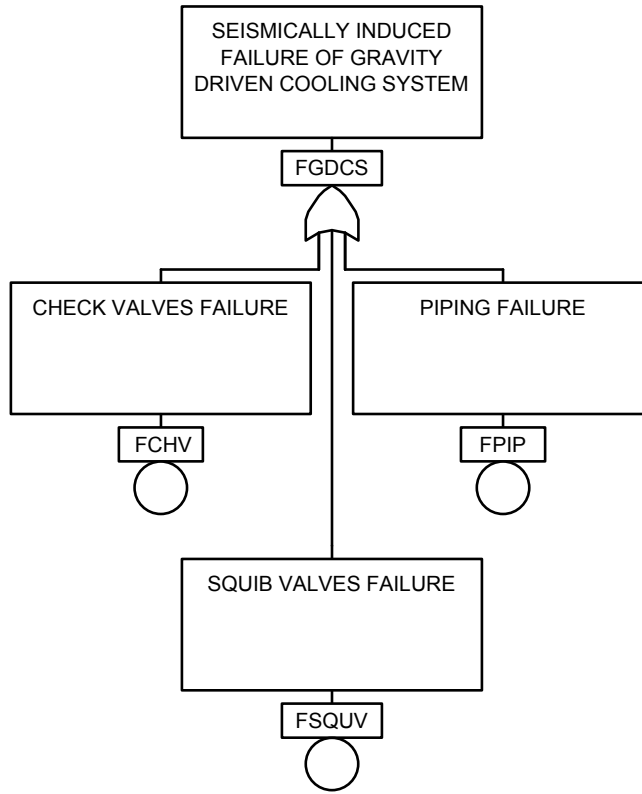


Figure 15-11. GDCS Seismic Fault Tree

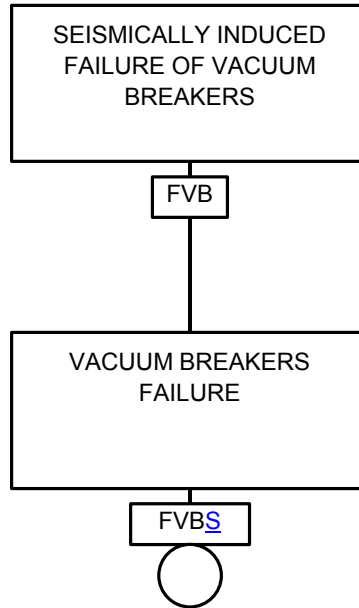


Figure 15-12. VB Seismic Fault Tree

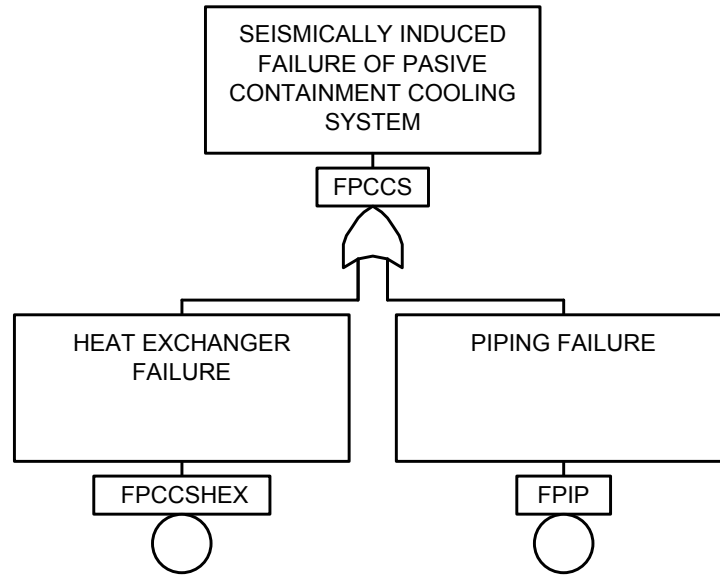


Figure 15-13. PCCS Seismic Fault Tree

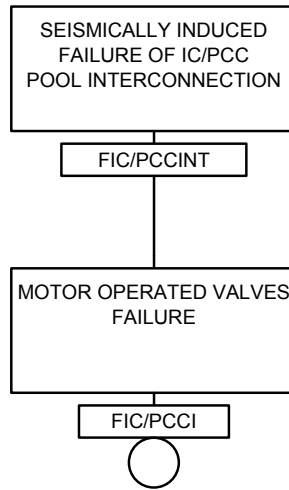


Figure 15-14. PI Seismic Fault Tree

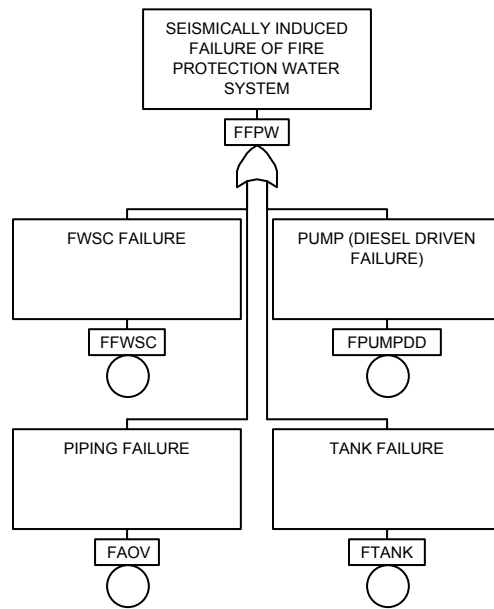


Figure 15-15. FPW Seismic Fault Tree

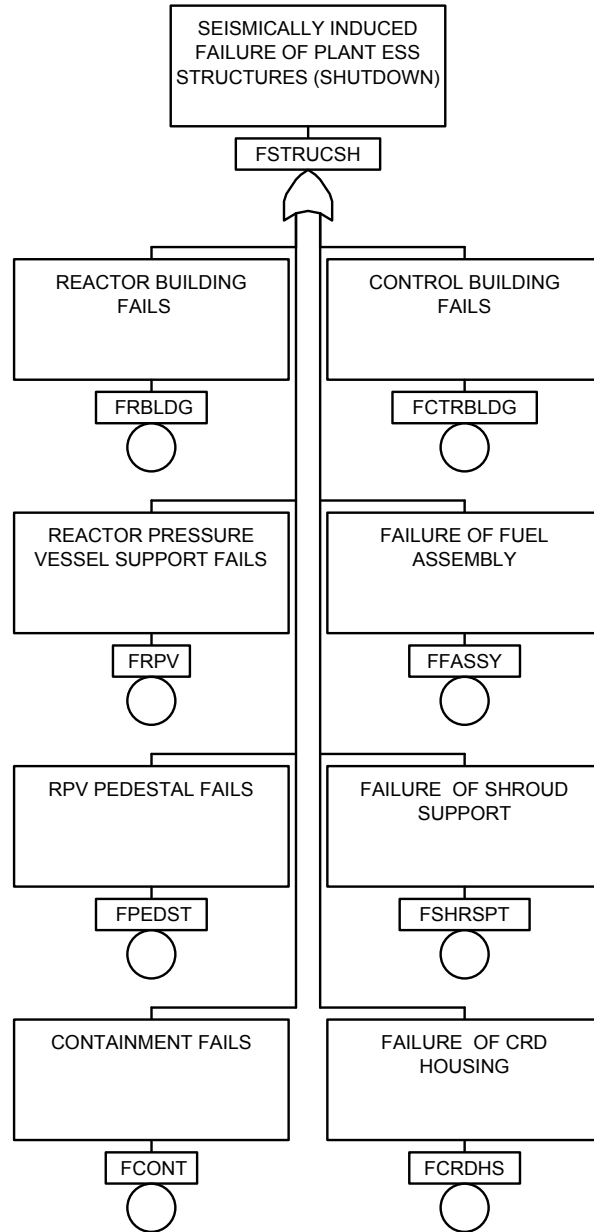


Figure 15-16. Structural Seismic Fault Tree (Shutdown Conditions)

SEISMIC EVENT	SIS	DC	IC	SRV	FPW	DPV	GDCS	FPW	Number	Class	Min-Max
LOPP during Mode 5 and Mode 5 Open	STRUCTURAL INTEGRITY-SHUTDOWN	DC POWER	ISOLATION CONDENSER	SRVs	FIRE PROTECTION SYSTEM	DPVs	GRAVITY DRIVEN COOLING	FIRE PROTECTION SYSTEM			
<pre> graph LR Root[] --- P1[] Root --- P2[] Root --- P3[] Root --- P4[] Root --- P5[] Root --- P6[] Root --- P7[] Root --- P8[] Root --- P9[] Root --- P10[] Root --- P11[] Root --- P12[] P1 --- FIC1[FIC] P2 --- FIC2[FIC] P3 --- FSRV[FSRV] P4 --- FSRV P5 --- FSRV P6 --- FSRV P7 --- FSRV P8 --- FSRV P9 --- FSRV P10 --- FSRV P11 --- FSRV P12 --- FSTRUCSH[FSTRUCSH] FIC1 --- FFPW1[FFPW] FIC2 --- FFPW1 FIC1 --- FDPV1[FDPV] FIC2 --- FDPV1 FSRV --- FFPW2[FFPW] FSRV --- FDPV2[FDPV] FFPW1 --- FGDCS1[FGDCS] FFPW2 --- FGDCS2[FGDCS] FGDCS1 --- FFPW3[FFPW] FGDCS2 --- FFPW3 P1 --- 1[1] P2 --- 2[2] P3 --- 3[3] P4 --- 4[4] P5 --- 5[5] P6 --- 6[6] P7 --- 7[7] P8 --- 8[8] P9 --- 9[9] P10 --- 10[10] P11 --- 11[11] P12 --- 12[12] </pre>									1		
									2		
									3		
									4	CD	0.84g
									5	CD	0.84g
									6		
									7		
									8	CD	0.84g
									9	CD	0.84g
									10		
									11	CD	0.84g
									12	CD	0.84g

Figure 15-17a. Seismic Event Tree – Shutdown Mode 5 and Mode 5 Open

NEDO-33201 Rev 3

SEISMIC EVENT	SIS	DC	IC	SRV	FPW	DPV	GDACS	FPW	VB	PCCS	PI	Number	Class	Min-Max
LOPP during Mode 5 and Mode 5 Open	STRUCTURAL INTEGRITY-SH UTDOWN	DC POWER	ISOLATION CONDENSER	SRVs	FIRE PROTECTION SYSTEM	DPVs	GRAVITY DRIVEN COOLING	FIRE PROTECTION SYSTEM	VACUUM BREAKERS	PASSIVE CONTAINMENT COOLING	IC/PCP POOL INTERCONNECT ION			
												1		
												2		
												3		
												4	CD	0.84g
												5	CD	0.84g
												6	CD	0.84g
												7	CD	0.84g
												8	CD	0.84g
												9		
												10	CD	0.84g
												11	CD	0.84g
												12	CD	0.84g
												13		
												14	CD	0.84g
												15	CD	0.84g
												16	CD	0.84g
												17	CD	0.84g
												18	CD	0.84g
												19		
												20	CD	0.84g
												21	CD	0.84g

Figure 15-17b. Seismic Event Tree – Shutdown Mode 5 and Mode 5 Open (Sensitivity)

SEISMIC EVENT	SIS	DC	FPW	GDCS	Number	Class	Min-Max
LOPP DURING MODE 6 UNFLOODED	STRUCTURAL INTEGRITY-SH UTDOWN	DC POWER	FIRE PROTECTION SYSTEM	GRAVITY DRIVEN COOLING			
					1		
					2		
					3	CD	0.84g
					4		
					5	CD	0.84g
					6	CD	0.84g

Figure 15-18. Seismic Event Tree – Shutdown Mode 6 Unflooded

S E I S M I C E V E N T	S I S	N u m b e r	C l a s s	M i n - M a x
L O P P D U R I N G M O D E 6 F L O O D E D	S T R U C T U R A L I N T E G R I T Y S H U T D O W N			
	F S T R U C S H	1		
		2	C D	0 . 8 4 g

Figure 15-19. Seismic Event Tree – Shutdown Mode 6 Flooded

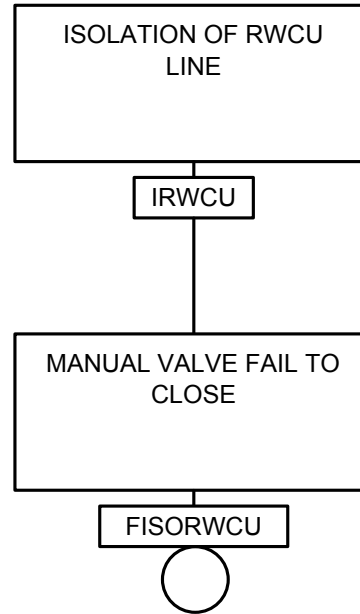


Figure 15-20. BOC In RWCU Line Fault Tree